

---

Electronic Theses and Dissertations, 2004-2019

---

2015

## Optimal distribution network reconfiguration using meta-heuristic algorithms

Arash Asrari  
*University of Central Florida*

 Part of the [Electrical and Electronics Commons](#)  
Find similar works at: <https://stars.library.ucf.edu/etd>  
University of Central Florida Libraries <http://library.ucf.edu>

This Doctoral Dissertation (Open Access) is brought to you for free and open access by STARS. It has been accepted for inclusion in Electronic Theses and Dissertations, 2004-2019 by an authorized administrator of STARS. For more information, please contact [STARS@ucf.edu](mailto:STARS@ucf.edu).

---

### STARS Citation

Asrari, Arash, "Optimal distribution network reconfiguration using meta-heuristic algorithms" (2015).  
*Electronic Theses and Dissertations, 2004-2019*. 52.  
<https://stars.library.ucf.edu/etd/52>

OPTIMAL DISTRIBUTION NETWORK RECONFIGURATION USING META-HEURISTIC  
ALGORITHMS

by

ARASH ASRARI

B.S. Shahid Bahonar University of Kerman, Kerman, Iran, 2008

M.S. Ferdowsi University of Mashhad, Mashhad, Iran, 2012

A dissertation submitted in partial fulfillment of the requirements  
for the degree of Doctor of Philosophy  
in the Department of Electrical Engineering & Computer Science  
in the College of Engineering and Computer Science  
at the University of Central Florida  
Orlando, Florida

Spring Term  
2015

Major Professor: Thomas Wu

© 2015 Arash Asrari

## ABSTRACT

Finding optimal configuration of power distribution systems topology is an NP-hard combinatorial optimization problem. It becomes more complex when time varying nature of loads in large-scale distribution systems is taken into account. In the second chapter of this dissertation, a systematic approach is proposed to tackle the computational burden of the procedure. To solve the optimization problem, a novel adaptive fuzzy based parallel genetic algorithm (GA) is proposed that employs the concept of parallel computing in identifying the optimal configuration of the network. The integration of fuzzy logic into GA enhances the efficiency of the parallel GA by adaptively modifying the migration rates between different processors during the optimization process. A computationally efficient graph encoding method based on Dandelion coding strategy is developed which automatically generates radial topologies and prevents the construction of infeasible radial networks during the optimization process.

The main shortcoming of the proposed algorithm in Chapter 2 is that it identifies only one single solution. It means that the system operator will not have any option but relying on the found solution. That is why a novel hybrid optimization algorithm is proposed in the third chapter of this dissertation that determines Pareto frontiers, as candidate solutions, for multi-objective distribution network reconfiguration problem. Implementing this model, the system operator will have more flexibility in choosing the best configuration among the alternative solutions. The proposed hybrid optimization algorithm combines the concept of fuzzy Pareto dominance (FPD) with shuffled frog leaping algorithm (SFLA) to recognize non-dominated suboptimal solutions identified by SFLA. The local search step of SFLA is also customized for power systems applications so that it automatically creates and analyzes only the feasible and

radial configurations in its optimization procedure which significantly increases the convergence speed of the algorithm.

In the fourth chapter, the problem of optimal network reconfiguration is solved for the case in which the system operator is going to employ an optimization algorithm that is automatically modifying its parameters during the optimization process. Defining three fuzzy functions, the probability of crossover and mutation will be adaptively tuned as the algorithm proceeds and the premature convergence will be avoided while the convergence speed of identifying the optimal configuration will not decrease. This modified genetic algorithm is considered a step towards making the parallel GA, presented in the second chapter of this dissertation, more robust in avoiding from getting stuck in local optimums.

In the fifth chapter, the concentration will be on finding a potential smart grid solution to more high-quality suboptimal configurations of distribution networks. This chapter is considered an improvement for the third chapter of this dissertation for two reasons: (1) A fuzzy logic is used in the partitioning step of SFLA to improve the proposed optimization algorithm and to yield more accurate classification of frogs. (2) The problem of system reconfiguration is solved considering the presence of distributed generation (DG) units in the network. In order to study the new paradigm of integrating smart grids into power systems, it will be analyzed how the quality of suboptimal solutions can be affected when DG units are continuously added to the distribution network.

The heuristic optimization algorithm which is proposed in Chapter 3 and is improved in Chapter 5 is implemented on a smaller case study in Chapter 6 to demonstrate that the identified solution through the optimization process is the same with the optimal solution found by an exhaustive search.

## **ACKNOWLEDGMENTS**

I would like to express my deepest appreciation to my supervisor, Dr. Thomas Wu, and my co-advisor, Dr. Saeed Lotfifard, for the patient mentorship they provided to me. Most especially, I would like to thank them for their excellent guidance, caring, support, and giving me the freedom to pursue my doctoral research in an excellent atmosphere under their supervision. I have learned a lot by working with them which has helped me recognize better my academic goals. Also, I would like to thank Dr. Michael Haralambous, Dr. Jennifer Pazour and Dr. George Atia as my committee members for their helpful comments on my proposal and this dissertation.

## TABLE OF CONTENTS

LIST OF FIGURES .....	viii
LIST OF TABLES .....	xi
CHAPTER ONE: INTRODUCTION.....	1
1.1 Adaptive parallel GA.....	3
1.2 Fuzzy Pareto dominance shuffled frog leaping algorithm .....	4
1.3 Dynamic fuzzy genetic algorithm .....	5
1.4 Adaptive fuzzy shuffled frog leaping algorithm .....	7
CHAPTER TWO : OPTIMAL DYNAMIC RECONFIGURATION OF LARGE-SCALE DISTRIBUTION SYSTEMS WITH TIME VARYING LOADS USING PARALLEL COMPUTING.....	10
2.1 Problem formulation .....	10
2.2 Chromosome encoding.....	12
2.3 Adaptive parallel GA .....	17
2.4 Reducing load condition scenarios using fuzzy C-mean classifier .....	19
2.5 Implementation.....	21
2.6 Simulation results and discussions.....	22
2.7 Summary .....	29
CHAPTER THREE: A HYBRID PARETO DOMINANCE BASED OPTIMIZATION METHOD FOR OPTIMAL DISTRIBUTION NETWORK RECONFIGURATION.....	31
3.1 Problem formulation .....	31
3.2 Fuzzy Pareto dominance algorithm.....	33
3.3 A reliability based network encoding.....	36
3.4 Shuffled frog leaping algorithm with adaptive local search .....	39

3.5 Implementation.....	45
3.6 Simulation results and discussions.....	47
3.7 Summary.....	55
CHAPTER FOUR: OPTIMAL DISTRIBUTION NETWORK RECONFIGURATION USING DYNAMIC FUZZY BASED GENETIC ALGORITHM .....	56
4.1 Overview of genetic algorithm.....	56
4.2 Determining crossover and mutation parameters.....	57
4.3 Simulation results and discussions.....	61
4.4 Summary.....	69
CHAPTER FIVE: THE IMPACT OF DISTRIBUTED GENERATION INTEGRATION ON OPTIMAL DISTRIBUTION NETWORK RECONFIGURATION.....	71
5.1 Methodology.....	71
5.2 Simulation results and discussions.....	77
5.3 Summary.....	86
CHAPTER SIX: EXHAUSTIVE SEARCH.....	87
CHAPTER SEVEN: CONCLUSION .....	92
LIST OF REFERENCES.....	94



## LIST OF FIGURES

Figure 1: (a) The corresponding tree for chromosome S1; (b) The corresponding tree for chromosome S1' .....	16
Figure 2: Schematic of the proposed adaptive parallel GA .....	18
Figure 3: 119-bus distribution network with aged and risky switches shown in red and thicker lines [49] .....	24
Figure 4 : The hourly load data of the studied year .....	25
Figure 5: The computed LCRI for each class .....	25
Figure 6: (a) Total fitness; (b) Number of Switching .....	26
Figure 7: The optimal network configuration for class #19 .....	27
Figure 8: Power loss values corresponding to class #19.....	28
Figure 9: The operation of initial tie switches .....	28
Figure 10: Pareto frontier identified by a typical Pareto-dominance algorithm .....	34
Figure 11: A radial network with two loops .....	37
Figure 12: The fuzzy functions calculating SRI for each switch.....	39
Figure 13: The sample network used to clarify the adaptive local search step.....	44
Figure 14: A 136-bus distribution network with 21 loops (Loop #16 contains branch numbers {1-7, 136, 73, 70, 63-68, 99-101, 103-107, 110, 153, 45-47, 43, 42, 40, 39}) [57] .....	47
Figure 15: The determined SRI of each switch .....	49
Figure 16: The number of AS members .....	50
Figure 17: The declining trend of average fitness values .....	51

Figure 18: The declining trend of fitness values ((a): average; (b): power loss; (c) voltage sag; (d) THD).....	53
Figure 19: The identified Pareto frontier .....	53
Figure 20: The fuzzy function determining P1 .....	59
Figure 21: The fuzzy function determining P2.....	60
Figure 22: The fuzzy function determining P3.....	61
Figure 23: Case study [62].....	62
Figure 24: The trend of the best fitness value in each generation .....	65
Figure 25: The trend of the average and the best fitness value in each generation .....	66
Figure 26: The final solution.....	67
Figure 27: The power loss of each branch .....	68
Figure 28: The trend of average fitness values .....	69
Figure 29: The flowchart of algorithm.....	72
Figure 30: A radial network with three loops .....	73
Figure 31: Updating the archive set members .....	74
Figure 32: Determining the fitness fuzzy value for classification .....	75
Figure 33: The case study [63].....	77
Figure 34: The number of AS members found by the algorithm.....	79
Figure 35: The declining trend of average voltage drop.....	80
Figure 36: The declining trend of average voltage sag.....	81
Figure 37: The frontiers identified by the algorithm for three scenarios .....	82
Figure 38: The voltage profile of configurations presented in Table 2 .....	83
Figure 39: The small case study for exhaustive search.....	87

Figure 40: The configuration with minimum power loss ..... 89

Figure 41: The configurations with (a): minimum voltage sag and (b): minimum THD ..... 90

## LIST OF TABLES

Table 1: Description of Added DG Units to the Network (Power Factor= 0.8 lag).....	23
Table 2: Performance of Different Scenarios .....	29
Table 3: Nonlinear Load Data (Percentage of Fundamental Frequency) .....	48
Table 4: Performance of Different Algorithms.....	52
Table 5: The Effect of the Proposed Reliability-based Encoding Strategy on the Performance of the Algorithm .....	55
Table 6: The Description of Different Scenarios .....	78
Table 7: The Configurations with the Lowest Voltage Drop .....	82
Table 8: The Configurations Located at the Center of Pareto Frontiers.....	84
Table 9: The Suboptimal Configurations Identified for Scenario #3 .....	85
Table 10: Branch Data of the Small Case Study.....	88
Table 11: Bus Data of the Small Case Study.....	88
Table 12: Nonlinear Load Data of the Small Case Study (Percentage of Fundamental Frequency) .....	88

## CHAPTER ONE: INTRODUCTION

Ever growing deployment of distribution automation (DA) technologies in distribution systems has made the skeleton of the power grids more flexible. The network topology can be dynamically reconfigured to optimally utilize the power grids. Distribution network reconfiguration is a common problem in distribution management systems which is proposed by Merlin and Back in 1975 [1]. Distribution network reconfiguration is the act of opening and closing the switching devices of power systems to reach a topology that optimizes the desired objectives.

Distribution systems reconfiguration has a variety of applications such as power loss reduction [2], load balancing [3], improving power quality [4], increasing distributed generation (DG) penetration [5], decreasing the number of switching operations [6], enhancing voltage stability margin [7], and system restoration [8].

The distribution automation usually aims at optimizing more than one objective function. There are mainly two techniques to solve multi-objective optimization problems: (1) Assigning different significance factors to the objective functions, adding them up and solving the optimization problem to optimize the resulted single function; (2) Adopting a Pareto dominance-based algorithm to provide a set of optimums instead of only a single solution. The advantage of the second option is that it provides alternative solutions. Therefore, the operator has more flexibility to select the best possible solution from the identified Pareto frontier based on the condition of the network.

The main challenge of implementing distribution network reconfiguration problem is the high number of different possible switching combinations in a network to be considered and analyzed as the candidates of the optimal configuration. That is why network reconfiguration is known as a combinatorial, non-linear, non-differentiable constrained optimization problem. Therefore, researchers have shown interest to employ meta-heuristic intelligent global optimization algorithms in order to solve this NP-hard problem. Examples of these evolutionary algorithms are genetic algorithm (GA) [9-10], partial swarm optimization (PSO) [11], harmony search algorithm (HSA) [12], honey bee mating optimization (HBMO) [13], tabu search algorithm (TSA) [14], ant colony optimization (ACO) [15], simulated annealing immune (SAI) [16], and artificial neural network (ANN) based algorithms [17-18].

This dissertation contains seven chapters. In the second chapter, an adaptive parallel GA is proposed to solve the problem of network reconfiguration when the time varying nature of electric load is taken into account. A Pareto based SFLA is proposed in the third chapter to resolve the main shortcoming of the presented method in Chapter 2. The proposed GA in Chapter 2 is improved in Chapter 4 to be able to automatically modify its parameters during the optimization process in order to enhance its efficiency in identifying more fertilized solutions. The proposed method in Chapter 3 is modified in Chapter 5 and the problem of network reconfiguration is solved in a smart grid in the presence of distributed generations (DGs). This chapter elaborates how the quality of suboptimal solutions will be affected when DG units are continuously added to the distribution network. The efficiency of the proposed method in Chapter 3, which is modified in Chapter 5, is verified by comparing the simulation results with an exhaustive search. Finally, Chapter 7 concludes this dissertation. The description of the

optimization methods proposed in this dissertation to solve the network reconfiguration problem for the aforementioned concerns are briefly described in the rest of this chapter.

### 1.1 Adaptive parallel GA

The distribution network reconfiguration, depending on how the load is modeled, can be dynamic or static. In static optimal distribution network reconfiguration, the loads are assumed to be one single constant value in entire optimization process. Although this assumption significantly reduces the computational burden of the algorithm, it cannot realistically model and cover the impacts of load variations. Therefore, the time varying nature of the loads needs to be taken into account [19-21]. For instance, in [22] to consider the impact of load variations a dynamic network reconfiguration method is proposed in which the optimization procedure is executed repetitively every hour as the load value varies.

Solving the optimization problem over a long period of time is computationally expensive; especially in large-scale distribution systems with a large number of switches and so many load condition scenarios. In order to address this issue, an intelligent and computationally efficient algorithm is proposed in the second chapter. Fuzzy C-Mean (FCM) is utilized to cluster the loading patterns into few clusters. This process significantly reduces the computational burden of the long run optimization procedure.

To efficiently encode the radial network topology, a method based on Dandelion encoding algorithm is developed. The proposed method assures that all the generated

chromosomes in the reconfiguration process automatically construct feasible radial configurations. This significantly improves the convergence speed of the algorithm as the tedious task of checking the radiality of the generated population is not needed any more.

In order to solve the optimization problem, a novel adaptive fuzzy-based parallel GA is proposed in which the migration rates among different processors are dynamically modified according to fuzzy rules. The proposed method reduces the computation burden of reconfiguration problem through parallel computing. Also, by developing an adaptive migration strategy based on fuzzy logic, it prevents the optimization algorithm from converging into local optimums.

The objective functions defined for the proposed method are power loss, number of switching and voltage drop. The strategy of assigning different significance factors is adopted to introduce one single objective function to the algorithm. The performance of the proposed reconfiguration method is demonstrated on a 119-bus distribution network.

## 1.2 Fuzzy Pareto dominance shuffled frog leaping algorithm

In the third chapter, a novel hybrid optimization model, which is a combination of fuzzy Pareto dominance (FPD) technique and shuffled frog leaping algorithm (SFLA), is proposed to identify a Pareto frontier as a set of high-quality suboptimal configurations for the network. SFLA is a meta-heuristic population based cooperative search method originated from natural memetics [23]. It provides a frog leaping rule for local search and a memetic shuffling rule for



global information exchange [24]. This global optimization algorithm is much faster in convergence compared to the other prominent evolutionary algorithms [25].

To consider the reliability of switching procedure, a reliability based frog coding is proposed in which a Switch Reliability Index (SRI) is defined for each switch. SRI is a fuzzy value between zero and one. A switch with a higher value of SRI has the higher chance to be selected for generating the initial population of the optimization process. Using the proposed reliability based frog coding, aged switches or the switches located at critical points of the network will be less participated in the process of network reconfiguration. Moreover, a systematic approach is proposed to adapt the local search step of SFLA for the application of distribution network reconfiguration so that only feasible frogs (i.e. radial configurations) are automatically born. This idea significantly increases the convergence speed of the conventional SFLA.

The objective functions to be optimized by the proposed algorithm are power loss, voltage sag and total harmonic distortion (THD) as two main indices of power quality. The strategy of Pareto dominance is utilized to recognize the suboptimal solutions identified by the optimization algorithm. The efficiency of the proposed method is verified on a large scale 136-bus electricity distribution network.

### 1.3 Dynamic fuzzy genetic algorithm

One of the most highly used methods in order to solve the network reconfiguration

optimization problem is genetic algorithm (GA). GA is a multi-dimensional and stochastic search strategy performing based on the idea of natural selection of chromosomes during the process of evolution. The main concentration of this algorithm is to set a reasonable trade-off between exploitation and exploration. If it focuses more on exploitation, the probability of getting stuck in a local optimum increases. On the other hand, higher exploration slows down the convergence process.

Therefore, there should be a meaningful interaction between the GA parameters (i.e. crossover probability and mutation probability) in order to boost the efficiency of GA performance [26]. For the purpose of identifying the optimal network configuration, GA is utilized in [27] in which the parameters are considered to be fixed values. In order to set a better balance between exploitation and exploration and avoid poor parameterization, researchers have proposed different techniques to determine the GA parameters dynamically as the algorithm proceeds and adjust them so that GA does not fall into local optimums while its convergence speed does not slow down. A "messy" approach is proposed in [28] to calculate and update the crossover and mutation probabilities based on the proportion of individual's fitness value and average fitness value compared to the best fitness value. A two-level adaptive system is proposed in [29] to dynamically determine and update the GA parameters "population size", "crossover rate", "mutation rate", "generation gap", "scaling window" and "selection strategy". The GA parameters are adopted in [30] based on the environmental constraint of maximum population size. In this technique, GA operators are considered as alternative reproduction strategies and fighting among individuals is permitted. A fuzzy logic controller (FLC) is proposed in [31] to adaptively tune the crossover rate based on the individuals' age in order to preclude the

premature convergence and improve the emulation of the biological process.

In the fourth chapter, the optimization problem of electric distribution reconfiguration is solved by a GA that employs three fuzzy functions to adaptively tune its crossover and mutation rates. The first fuzzy rule is defined based on the position of each chromosome compared to the best chromosome in the same generation. The second fuzzy rule is introduced on the basis of the situation of all the chromosomes compared to the best chromosome in the same generation. The output of the third fuzzy rule depends on the lifetime of each chromosome. Defining these three fuzzy functions, the probability of crossover and mutation changes as the algorithm proceeds and the premature convergence is avoided while the convergence speed of identifying the global optimal configuration does not decrease.

#### 1.4 Adaptive fuzzy shuffled frog leaping algorithm

The concentration of the fifth chapter is to analyze a potential smart grid solution to more high-quality suboptimal configurations of distribution networks. This new paradigm of electrical grids proposes the adoption of two-way flows of electricity and builds a distributed energy delivery network. As a result, utilities are enforced to evolve their classical topologies to accommodate distributed generation (DG). DG units are categorized in two main groups: (1) conventional generation resources such as gas turbines, diesel generators, fuel cells, and battery banks; (2) renewable energy resources such as wind turbines, solar cells, hydro power, and hybrid wind-PV-battery system. The idea of decentralized generation suggests the generation of

electricity from many small energy resources with the purpose of improving the security of supply and decreasing the environmental impacts of excessive burned fossil fuels in central plants.

Considering the noticeable growing trend of on-site generation units in distribution systems over the last years, researchers have shown interest to solve the problem of network reconfiguration in the presence of DGs. In [32] a particle swarm optimization (PSO) algorithm is presented to solve network reconfiguration problem with the purpose of maximizing DG integration and minimizing total power loss. A meta-heuristic harmony search algorithm (HSA) is employed in [33] to simultaneously solve the optimal DG placement and network reconfiguration problems to optimize power loss and voltage profile. Optimal locations of DG units are recognized by sensitivity analysis in this study. A genetic algorithm is utilized in [5] to reconfigure distribution systems so that it maximizes the penetration of DG units while it optimizes voltage profile and thermal constraints (i.e. total loading of the branches). In [34] operation strategies are taken into account to utilize network reconfiguration of automated distribution systems in the presence of DGs as a real-time operation to optimize power loss and service restoration. An artificial bee colony (ABC) algorithm is presented in [35] to optimally reconfigure a distribution network containing hybrid renewable systems (wind turbines & solar cells) as DGs so that the total power loss, the total electrical energy cost, and the total reduced emission of atmospheric pollutants are optimized.

A Pareto-based global optimization algorithm is proposed in the fifth chapter to solve the multi-objective problem of distribution system reconfiguration with the purpose of optimizing

voltage profile and voltage sag. The optimization method utilizes a Pareto dominance technique to recognize non-dominated solutions identified by SFLA which is adapted in the encoding and partitioning steps. Developing this Pareto-based optimization technique, the system operator will not have to rely on only one single solution. The algorithm will identify a set of high-quality suboptimal solutions on the Pareto frontier which are unable to dominate each other. Any of the recognized solutions on the Pareto frontier might be adopted as a candidate network configuration based on the situation of system. A fuzzy logic is introduced in the partitioning step of SFLA based on the values of voltage drop and voltage sag in order to provide a more accurate criterion for the classification of frogs.

# CHAPTER TWO : OPTIMAL DYNAMIC RECONFIGURATION OF LARGE-SCALE DISTRIBUTION SYSTEMS WITH TIME VARYING LOADS USING PARALLEL COMPUTING

## 2.1 Problem formulation

In this chapter the following objectives are selected for optimal network reconfiguration:

(1) power losses; (2) voltage deviation from the nominal value; and (3) the number of switching.

$$Max (k_1 * fit_1(\sum_{i=1}^C \frac{D_i}{365} \cdot F_1^i) + k_2 * fit_2(\sum_{i=1}^C \frac{D_i}{365} \cdot F_2^i) + k_3 * fit_3(\sum_{k=1}^K \sum_{j=1}^C \sum_{i=1}^C N_{ij} \cdot w_k \cdot x_{ij}^k)) \quad (1)$$

$$F1 = \sum_{f=1}^{Nf} \sum_{l=1}^m Ploss_f^l \quad (2)$$

$$Ploss_f^l = r_f^l \frac{(P_f^l)^2 + (Q_f^l)^2}{|V_f^l|^2} \quad (3)$$

$$F2 = \sum_{n=1}^N |V^{\max} - V_n| \quad (4)$$

*Subject to*

$$V^{\min} \leq V_n \leq V^{\max} \quad (5)$$

$$I_l \leq I_l^{\max} \quad (6)$$

$$m = N - n_s \quad (7)$$

$$A.I = L \quad (8)$$

where, the dynamics are  $i, j$  and  $k$ .  $i$  and  $j$  count the number of clusters (classes). And  $k$  refers to the switch number.  $C$  represents the total number of clusters. The concept based on which clusters are defined will be explained in Section 2.4.  $P_{loss}_f^l$  denotes the line loss of branch  $l$  in feeder  $f$ .  $P_f^l, Q_f^l, V_f^l$  and  $r_f^l$  stand for the active power, reactive power, voltage and the resistance value of the head node of feeder  $f$  and branch  $l$ , respectively.  $V_n, I_l$  and  $I_l^{\max}$  represent the voltage of bus  $n$ , the current of branch  $l$  and the maximum allowed value of  $I_l$ , respectively.  $F_1^i$  and  $F_2^i$ , respectively, refer to F1 and F2 for the loading condition at class  $i$ .  $D_i$  is the number of days that are assigned to cluster  $i$ .  $N_{ij}$  signifies the total number of transitions from class  $i$  to class  $j$  in the year under study.  $x_{ij}^k$  is a binary variable with the default value of zero. If in the transition from class  $i$  to  $j$  the status of switch  $k$  is changed, the value of  $x_{ij}^k$  becomes one. That is why this variable represents the connectivity of the relevant switch (branch).

A weighting factor of  $w$  is assigned to each switch based on how much a given switch is desired to participate in the process of network reconfiguration. For instance, the assigned value of  $w$  to a given switch could be increased according to asset management monitoring data as the switch ages. Therefore, the possibility of participation of that switch in the reconfiguration process reduces. Another scenario could be a case when a given switch is located at a critical location of the network and changing its status is not desirable as it may cause disturbances that are not tolerable by adjacent sensitive loads or it might lead to loss of a significant portion of the network. In these cases also a higher value can be assigned to  $w$  associated to the switch.

$K$  stands for the total number of switches.  $m, N_f, N$  and  $n_s$  are the total number of branches, feeders, nodes (buses) and energy sources, respectively.  $I$  is the  $m$ -vector complex

branch current,  $L$  is the  $n$ -vector complex nodal current, and  $A$  is the  $n \times m$  node-to-branch incidence matrix.  $k_1$ ,  $k_2$  and  $k_3$  are weighting factors for power loss, voltage deviation and number of switching which are defined by the operator based on the relative importance of the corresponding objective. For instance, if the main concentration of the operator is on the minimization of power loss, a higher value is assigned to  $k_1$  (e.g.  $k_1=0.7$ ,  $k_2=0.2$ ,  $k_3=0.1$ ).  $fit_1$ ,  $fit_2$  and  $fit_3$  are the relevant fuzzy membership functions defined by operator to scale and restrain the variables between zero and one. These functions should be defined so that maximizing the output of these functions is equivalent to minimizing their corresponding arguments (i.e. power loss, voltage deviation or switching number). For example, if  $\sum_{i=1}^C \frac{D_i}{365} \cdot F_1^i = 0$  then,  $fit_1(\sum_{i=1}^C \frac{D_i}{365} \cdot F_1^i)$  should be equal to one.

## 2.2 Chromosome encoding

Efficient distribution network topology encoding significantly reduces the computational burden of the optimization procedure. The most straightforward but the least efficient encoding method is constructing a string formed by the binary status of the switches (closed/open) [10]. This technique requires an extra function to be integrated into the GA structure to check the radiality of network topology. A distribution network is called radial when there is only one path between each node (bus) and the source (Node #1). A vertex encoding method based on the Prüfer number is presented in [36] in order to avoid the tedious radiality check procedure of GA. This strategy relies on the number of nodes (i.e. buses) in the network instead of the number of



switches or branches. An edge-set encoding based algorithm is proposed in [37]. The bits of each chromosome, generated by this method, refer to the branch numbers that are connected together directly or indirectly. A Matroid theory based GA encoding algorithm is proposed in [10] in order to solve the network reconfiguration problem faster without checking the distribution network radiality. In [38] an analytic comparison of six classical tree graph encoding techniques (i.e. characteristic vector, Prufer numbers, network random keys, edge sets, node biased encoding, and link and node biased encoding) are provided. The performance of GA using each of these encoding strategies has been analyzed as well. Two sequential encoding techniques called subtractive and additive are proposed in [9] to generate radial topologies for solving network reconfiguration problem. An encoding method based on the Prufer number and a clustering string is presented in [39] for solving optimal spanning tree problem in communication systems.

The power distribution systems encoding/decoding method not only should generate radial configuration but also needs to prevent “infeasible radial network” that refers to the generated topologies in which the buses with no switch in between are connected together. Moreover, the implementation of the coding strategy should not be too complicated.

Dandelion coding method is proposed in [40] to encode spanning trees in communication systems. Dandelion strategy is one of the most computationally efficient encoding techniques for spanning trees. This coding scheme exhibits a noticeably higher locality and heritability compared to the other encoding strategies like Blob code, Prufer code and direct tree code [40]. Furthermore, if the problem size increases, its locality improves as well. These features make this method very appropriate for large-scale networks.

In this chapter the problem of finding the optimal radial topology is formulated as identifying the optimal feasible spanning tree. It should be mentioned that “tree” and “radial network” refer to the same concept in this dissertation. A network encoding algorithm based on Dandelion theory is developed for the application of electrical distribution networks that generates "Radial & Feasible" structures. The procedure for implementing the encoding strategy is as follows:

0) Set  $k=0$ ;

1) Randomly generate vector  $S1$  containing  $n-2$  components whose elements are selected from the set  $\{1,2,\dots,n\}$  where  $n$  refers to the number of nodes;

2) Develop matrix  $S2$  whose second row is  $S1$ , and the first row is the vector  $[2, 3,\dots,n-1]$ ;

3) Switch the first and second row of  $S2$  and call the generated matrix  $S3$ . Then, build vector  $S4$  whose components are the common columns in  $S2$  and  $S3$ ;

4) Sort the components of  $S4$  in a descending order, delete the repetitive components and call the generated vector  $S5$ ;

5) In order to keep the radial topology of the distribution network with multiple feeders, connect all the root nodes (substations) to each other with a “virtual line”.

6) Connect the nodes of  $S5$  to each other. Then, connect node 1 to the first component of  $S5$ , and node  $n$  to the last element of  $S5$ . Finally, connect the elements in the first row of  $S2$  to the corresponding components existing in the second row of  $S2$ .

7) The generated chromosome using this node-based coding is always radial. However, after constructing the radial chromosome its feasibility should be checked in this

*step. If the generated chromosome is feasible, set  $k=k+1$ . It is notable this branch checking process takes considerably less time in comparison to the checking of radiality of the chromosomes in conventional binary coding.*

*8) If the generated tree in the previous step is feasible, remove the virtual line and the developed chromosome will be still radial.*

*9) If  $k$  is equal to the desired number of population, go to 10; otherwise go to 1.*

*10) Finish.*

The following example explains the encoding method numerically. Consider a network with  $n=9$  nodes:

***Step 1)***

$$S1 = [5 \ 6 \ 8 \ 2 \ 6 \ 4 \ 9] \quad (9)$$

***Step 2)***

$$S2 = \begin{bmatrix} 2 & 3 & 4 & 5 & 6 & 7 & 8 \\ 5 & 6 & 8 & 2 & 6 & 4 & 9 \end{bmatrix} \quad (10)$$

***Step 3)***

$$S3 = \begin{bmatrix} 5 & 6 & 8 & 2 & 6 & 4 & 9 \\ 2 & 3 & 4 & 5 & 6 & 7 & 8 \end{bmatrix} \quad (11)$$

$$S4 = \{(2,5), (5,2), (6,6)\} \quad (12)$$

***Step4)***

$$S5 = \{2, 5, 6\} \tag{13}$$

**Step 5)** It is assumed there is only one substation in the network. Therefore, there is no need to consider the virtual links.

**Step 6)** Figure 1 (a) depicts the corresponding tree to chromosome S1. As it can be realized from the figure, a unique tree can be assigned to any other chromosome using this encoding technique.

**Step 7)** According to Figure 1 (a), the generated tree for S1 is feasible. In this example, it is assumed that only the adjacent nodes can be connected together.

Now if the same procedure is repeated for the initial random vector  $S1' = \{9, 3, 1, 7, 8, 5, 3\}$ , one can attain the relevant tree illustrated in Figure 1 (b). In this radial network, the connections between 1-7, 3-9, 9-2, and 8-3 are not possible which makes this tree an infeasible distribution network. Therefore, in Step 7 the created vector is removed from the initial population of the optimization procedure.

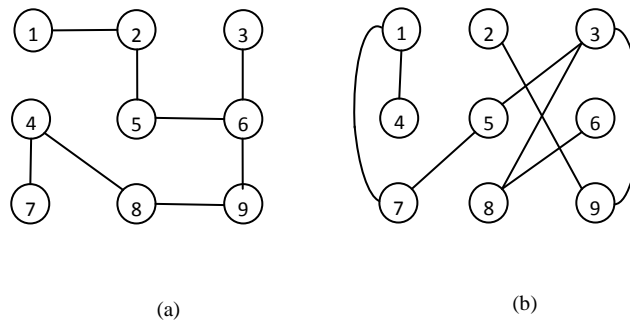


Figure 1: (a) The corresponding tree for chromosome S1; (b) The corresponding tree for chromosome S1'

### 2.3 Adaptive parallel GA

Parallel Genetic algorithms (PGAs) are considered as a class of guided random evolutionary algorithms [41]. While PGAs still have the benefits of serial GAs (i.e. robustness, easy customization for new problems, and multiple solution capabilities), they also have higher efficiency (i.e. super numerical performance) [42], larger diversity maintenance [43], additional availability of CPU [44], and higher speed in comparison to serial GAs. The PGAs can be categorized into three general groups: (1) Master-slave PGA; (2) Fine-grained PGA; (3) Multi-deme PGA. In a master-slave PGA, there is only one united population in which the evaluations of chromosomes are distributed by scheduling fractions of population among different processing slave units. A fine-grained PGA contains only one spatially structured population. Selection and mating in this method are limited to small groups to avoid groups' overlapping and disseminating better individuals across the entire population. A multi-deme PGA contains several populations that exchange their chromosomes occasionally based on a process called migration. More details about these three PGA approaches can be found in [45].

One important factor that has a direct impact on the performance of multi-deme PGA is the utilized migration strategy. In conventional methods the migration rate is a predefined fixed value. However, as optimization is a dynamic process, developing adaptive migration rate that is dynamically calculated and updated based on the current status of different demes, will improve the algorithm in terms of speed and quality of final result.

Figure 2 depicts the proposed adaptive parallel GA. After each certain number of generations, an adaptive migration strategy based on a fuzzy logic is applied to dynamically

assign different migration rates among processors. This migration rate is calculated based on the similarity between each two processors. The migration rate increases as the similarity reduces. The similarity is defined based on the difference between the objective values of different processors. This adaptive method provides more satisfactory results compared to the conventional migration technique in which a predetermined number of chromosomes are allowed to migrate between the neighboring processors in each step. The proposed adaptive migration strategy increases the convergence speed of the parallel computing procedure by adaptively increasing the chance of migration between the processors with lower similarity.

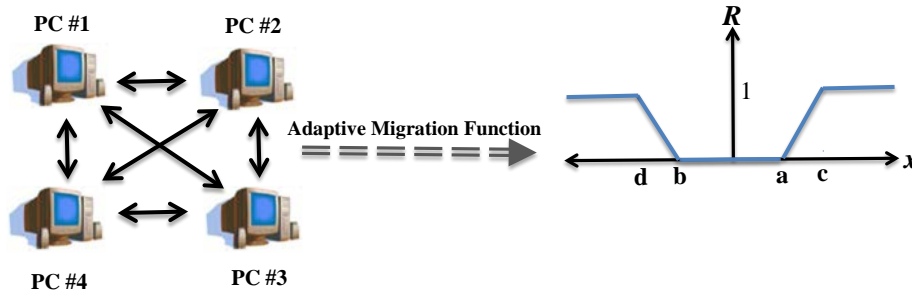


Figure 2: Schematic of the proposed adaptive parallel GA

Equation 14 represents the general form of the fuzzy logic used in Figure 2 that dynamically calculates the migration rate between PC#2 and PC#3.

$$R(x) = \begin{cases} 0 & b \leq x < a \\ \frac{x-a}{c-a} & a \leq x < c \\ \frac{x-b}{d-b} & d \leq x < b \\ 1 & x \geq c \parallel x \leq d \end{cases} \quad (14)$$

where,  $x$  stands for the absolute difference value between the average fitness values of PC #2 and PC #3. A higher difference value causes a more crowded population of migrating chromosomes between the corresponding PCs. In Equation 14 a higher difference value of a-c or b-d increases the diversity in the migration procedure. Therefore, it is a trade-off between not falling into local optimums and the spread of convergence.

At a later stage, the computed migration rate ( $R$ ) is multiplied by the maximum allowed number of transferring chromosomes to attain the number of individuals to be exchanged between these two PCs. The same procedure is carried out for every two other PCs.

After determining the number of migrating chromosomes, a systematic strategy should be employed to select the chromosomes which need to be migrated. Randomly selecting the chromosomes may prevent selecting the most fertilized individuals for the migration. On the other hand, selecting the chromosomes with highest objective values may lead to immature convergence and trapping the algorithm in local minima. To address this issue, the roulette-wheel selection technique [46] is utilized in the proposed migration strategy. In this method, the chromosomes with higher objective values have a higher chance to be selected for the migration process. However, there is still a chance for the less fertilized individuals to be migrated with the hope of transferring the new and rare features (genes) to the other PCs.

#### 2.4 Reducing load condition scenarios using fuzzy C-mean classifier

In the proposed optimal distribution network reconfiguration method, the time varying

nature of the loads is taken into account. However, performing the optimization algorithm for every possible load condition scenario is not computationally practical. To address this issue, the load scenarios are reduced by clustering the daily load data. Fuzzy C-Mean (FCM) algorithm [47] is utilized for this classification purpose. One of the most significant advantages of this clustering technique is that it provides more accurate results for overlapped nontrivial samples compared to other clustering techniques such as k-means algorithm [48].

In this method, the desired number of classes as well as initial clustering seeds is determined in the first stage. This algorithm updates the location of seeds (daily load curves) in each iteration and then a fuzzy membership vector, containing the degrees of membership to each of the clusters, is assigned to each seed. The membership degrees are assigned based on the distance between each seed and the centers of other clusters. The highest membership degree (i.e. the least distance value) in each fuzzy vector indicates the corresponding class of the relevant daily load curve. The required procedure to implement FCM method is detailed in [47].

In the proposed optimal reconfiguration algorithm, once the daily load data over the studied year are classified using FCM classifier, Load Class Representative Index (LCRI) is defined as the average value of each class which is used as the representative of each class in the process of the optimization.

Using the employed load scenario reduction method, the 365 daily load data are reduced to only  $M$  LCRI values which significantly reduces the computational burden of the optimization process.



## 2.5 Implementation

The following pseudo code represents the implementation procedure of the proposed algorithm.

1) *Apply FCM classifier algorithm to the existing 365 daily load curves of the studied year.*

2) *Put Day\_counter=1.*

3) *If the optimal configuration of Class (Day\_counter) has been already determined, put Day\_counter= Day\_counter +1 and go to step 2; otherwise, go to step 4.*

4) *Calculate the corresponding LCRI (Class(Day\_counter)), and consider that value as the electricity demand of the network.*

5) *Create N radial and feasible structures, through implementing the ten steps elaborated in section 2.2, as the initial population of GA.*

6) *Locate the N chromosomes in different PCs equally. Implement the following steps for all the PCs in parallel.*

7) *Put Generation=1.*

8) *Run the power flow algorithm and calculate the fitness value for each chromosome using Equations 1-4 provided in section 2.1.*

9) *Apply the adopted selection operator to determine the individuals participating in the mating pool.*

10) *Apply the selected crossover and mutation strategies to specify the chromosomes taking part in the next generation.*

11) If  $[Generation/Migration\_gap]$  equals an integer value, apply the proposed adaptive fuzzy based migration strategy to determine the number of chromosomes to be transferred between each two parallel processors. Otherwise, go to step 13.

12) Apply the roulette-wheel selection technique to select the individuals to be transferred mutually between each two processors.

13) If  $Max\_Generation=Generation$ , go to step 14. Otherwise,  $Generation=Generation+1$  and go to step 8.

14) Print the identified individual with the highest fitness value in all the PCs as the best configuration of the corresponding class.

15) If  $Day\_counter=365$ , go to step 16. Otherwise,  $Day\_counter=Day\_counter+1$  and go to step 3.

16) Finish.

## 2.6 Simulation results and discussions

The proposed algorithm is implemented in MATLAB software on a computer with the processor of Intel(R) Xeon(R) CPU E5-2603 0 @ 1.80 GHz. The network shown in Figure 3 is selected as a platform for implementing the algorithm. It is a 119-bus distribution network presented in [49] with a difference that five distributed generation (DG) units are added to the system. The tie switches are numbered and presented with dash lines. Table 1 presents the location and the capacity of the added DG units.

As it was mentioned in 2.1, a weighted sum of three different fitness values is optimized in this chapter. In this study,  $K_1$ ,  $K_2$ , and  $K_3$  are assumed to be equal (i.e. 0.333), which means all the three fitness values have the same importance in the optimizing process.

Table 1: Description of Added DG Units to the Network (Power Factor= 0.8 lag)

	<b>DG1</b>	<b>DG2</b>	<b>DG3</b>	<b>DG4</b>	<b>DG5</b>
Bus No.	27	56	65	94	118
Output (MW)	0.1	0.15	0.3	0.2	0.2

In Figure 3, the aged switches or the switches that are located at sensitive locations are presented with red and thicker lines. As it was discussed in section 2.2, these switches are desired not to participate in the reconfiguration process. To reach this goal, the operator can simply assign a higher value of  $w$  in Equation 1 for the aged or more critical switches.

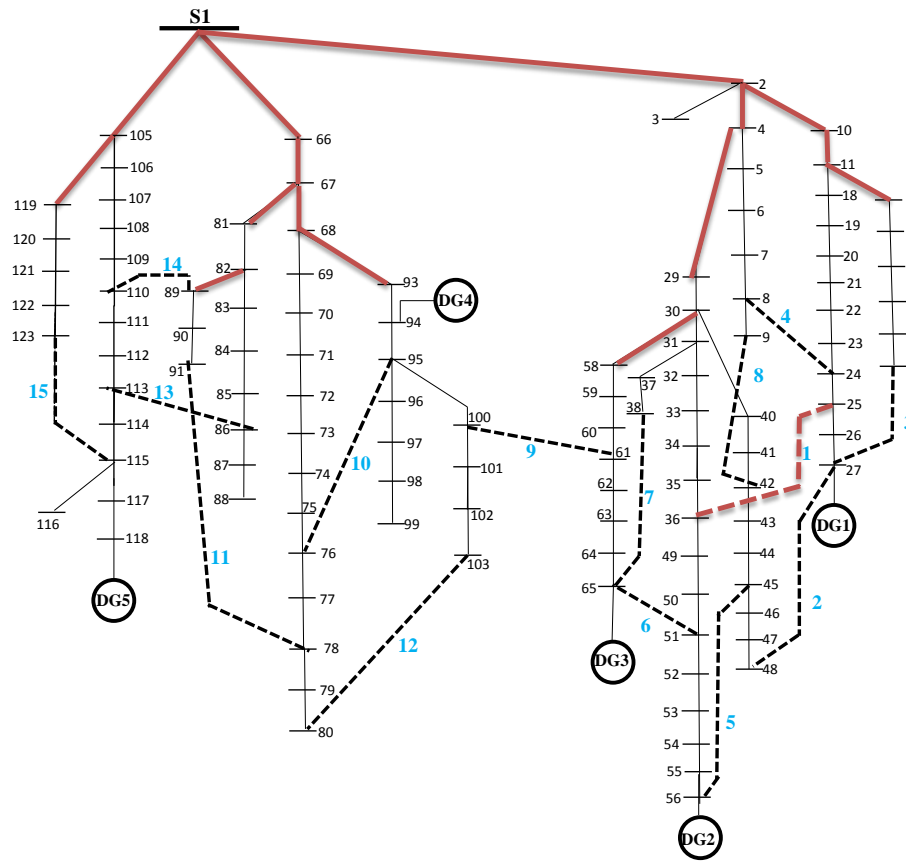


Figure 3: 119-bus distribution network with aged and risky switches shown in red and thicker lines [49]

The assumed hourly load of the studied network over a year is depicted in Figure 4. For this application, FCM is implemented to classify the daily load curves into 20 ( $M=20$ ) classes. The computed LCRI together with the number of days belonging to each class are presented in Figure 5. For example, the class no. 4 has the highest value of LCRI (7023.9 MW). This class represents 16 days of the year. Once the optimization problem is solved, a certain optimal configuration is found for each day of the year. For example, the class no. 19 contains 15 daily load curves related to days #186, 190-191, 196-197, 199-201, 204-207, and 211-213. It means that the configuration identified by the optimization algorithm for class #19 is utilized for the

mentioned days. It is notable that the assumption in this dissertation is that the future load data are already predicted.

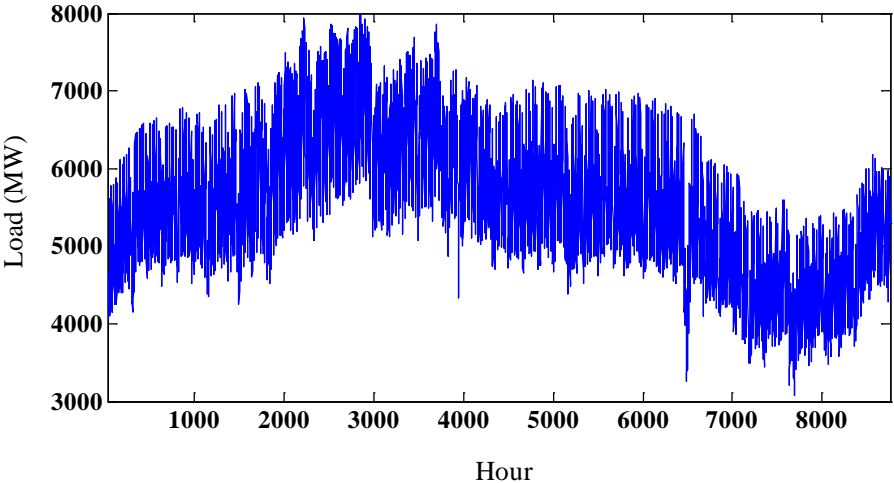


Figure 4 : The hourly load data of the studied year

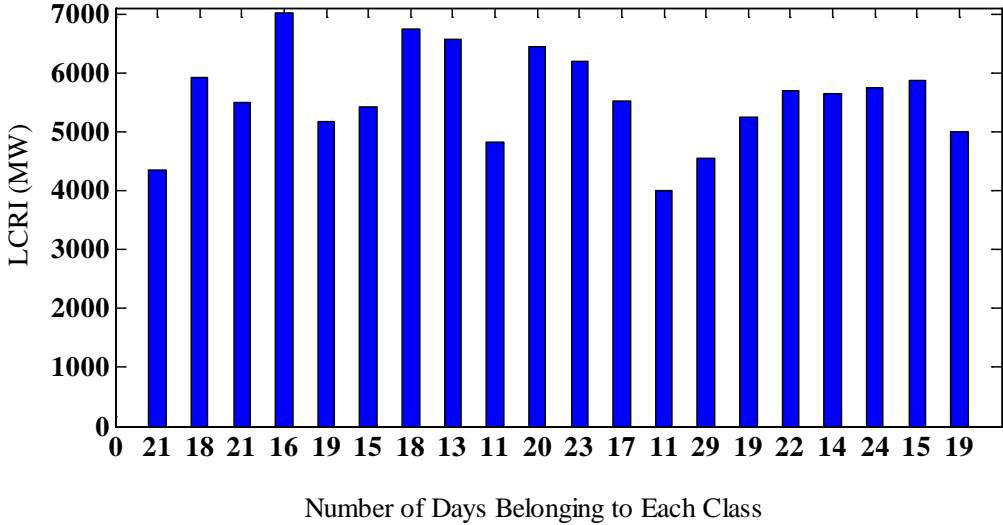


Figure 5: The computed LCRI for each class

The proposed parallel GA model is implemented on four processors each of which containing 100 chromosomes. It is assumed that after each 10 iterations (i.e. migration gap), the adaptive fuzzy migration strategy, discussed in section 2.3, is carried out among all the processors. Figure 6 illustrates the increasing trend of the total fitness value as well as the declining trend of number of switching for the four parallel PCs during 30 generations. According to Figure 6, PC #3 identifies the most fertilized solution because of its efficient migrations at iteration #10 and #20.

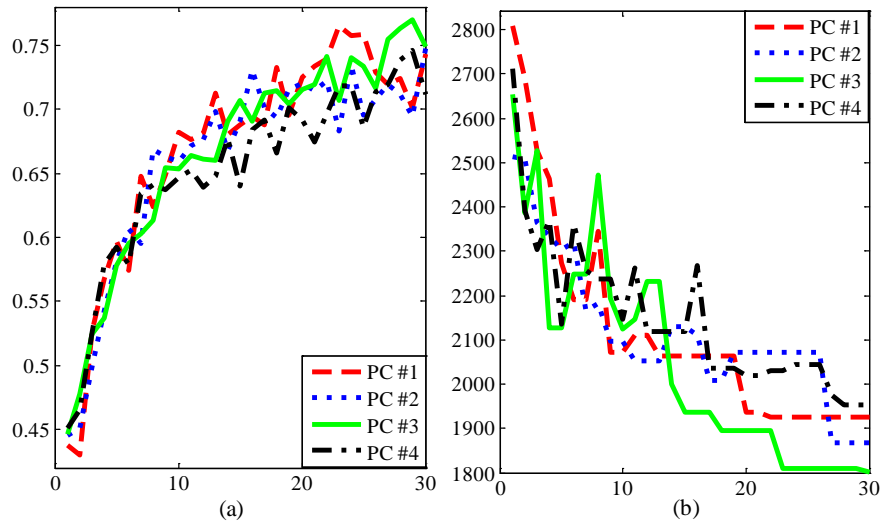


Figure 6: (a) Total fitness; (b) Number of Switching

The configuration identified by the optimization algorithm for class #19 is presented in Figure 7. The operator should apply this configuration at the days corresponding to class #19. The open switches for this configuration are shown by red and bold dash lines. It is notable that, the status of the aged and risky switches has not been changed as it was desired.

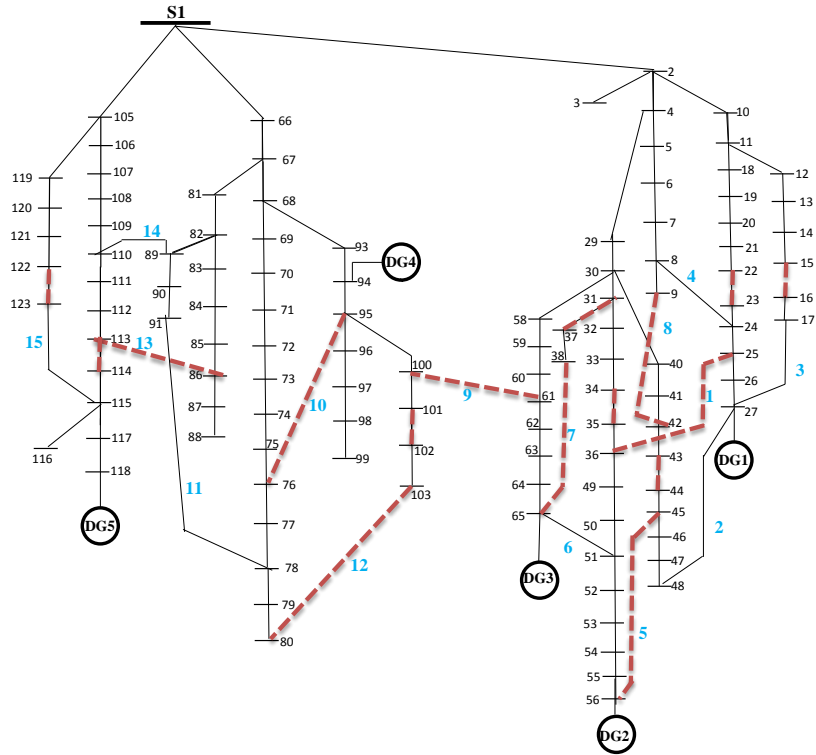


Figure 7: The optimal network configuration for class #19

Figure 8 illustrates how the power loss of each branch changes after optimal reconfiguration of the network for class# 19. According to Figure 8, the branch power loss values significantly reduce in the identified network configuration.

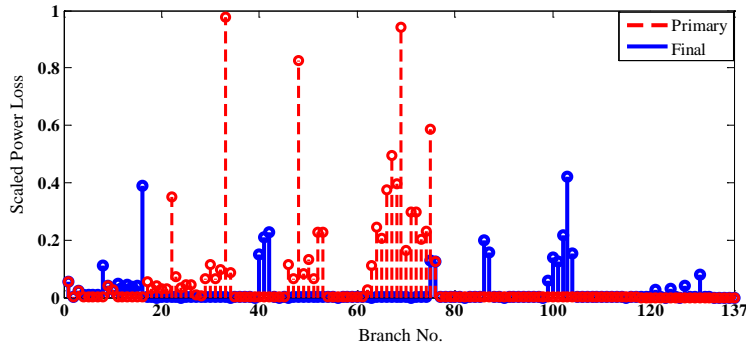


Figure 8: Power loss values corresponding to class #19

The schedule of all the initial tie switches over the studied year is illustrated in Figure 9. The vertical axis presents the number of classes in which the corresponding tie switch will be closed. According to this figure, the status of tie switches #9 and #1 do not change at all (stay open) and the status of switch #3, 4 and 13 stay the same (closed) in most classes.

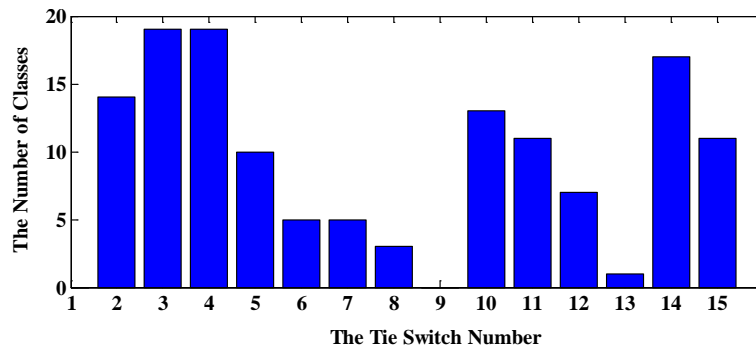


Figure 9: The operation of initial tie switches

Finally, the performance of the proposed algorithm is compared with that of GA with only one PC (i.e. parallelism is not used) and conventional parallel GA without the fuzzy migration (i.e. migration rate is a fixed predefined number), as is shown in Table 2. This table



shows the superior performance of the proposed method over the others. The word “primary” refers to the original network (Figure 3) before applying any reconfiguration. The proposed PGA reduces the power losses the most with the minimum number of switching and keeps the voltage of the weakest bus of the network closer to 1 per unit. As it was expected, conventional single GA has a considerably higher computational burden compared to the corresponding parallel-based GAs.

Table 2: Performance of Different Scenarios

	<b>Primary</b>	<b>Proposed PGA</b>	<b>Single Processor GA</b>	<b>Conventional PGA</b>
Number of PCs	-	4	1	4
Migration method	-	Fuzzy	-	Fix
Power loss (MW)	1474.10	1126.31	1155.14	1141.48
$V_{\min}$	0.9572	0.9709	0.9682	0.9693
No. Switching	0	1494	1760	1694
Computational Burden (S)	-	73448	252723	72360

## 2.7 Summary

In this chapter a novel optimization power distribution reconfiguration method is

proposed that identifies the high-quality suboptimal feasible topologies for large-scale networks with time varying loads. The proposed method can tackle the computational burden of large-scale power distribution systems reconfiguration by using parallel processing, efficient topology encoding, and load scenario reduction. Fuzzy based migration strategy is proposed to dynamically compute the number of fertilized chromosomes that should be migrated among the processors of parallel GA. A modified Dandelion encoding is developed that reduces the computational burden of classic binary coding strategy by automatically generating feasible and radial topologies during the optimization process. An FCM clustering method is adopted to decrease the considerable amount of load scenarios during the year under study.

One of the main advantages of the proposed dynamic power distribution systems reconfiguration method is that the optimization process is carried out over a long period of time in contrast to the existing methods that the optimization is re-executed every short period of time. Therefore, by using the proposed method the accumulated objective functions are optimized.

# CHAPTER THREE: A HYBRID PARETO DOMINANCE BASED OPTIMIZATION METHOD FOR OPTIMAL DISTRIBUTION NETWORK RECONFIGURATION

## 3.1 Problem formulation

The objective functions that are optimized in this chapter are as follows:

A) Power loss: The total active power wasted in a network is calculated by using Equations 2 and 3.

B) Voltage sag: According to IEEE standard 1159-1995, voltage sag is defined as a decrease to between 0.1 and 0.9 p.u. in root mean square value of voltage signal at the power frequency for durations of 0.5 cycle to 1 min [50]. In order to consider the worst cases, three-phase short circuit current faults are used to calculate voltage sag. The sagged voltage is computed for the buses called points of common coupling (PCC) which are determined by the system operator. The following equation computes the total voltage sag in a radial distribution network.

$$F2 = \sum_{i=1}^{N_{PCC}} \sum_{j=1}^N V_{i,j}^{sag} = \sum_{i=1}^{N_{PCC}} \sum_{j=1}^N \left| \frac{z_{ij} + z_f}{z_s + z_{ij} + z_f} \right| \quad (15)$$

where,  $V_{i,j}^{sag}$  signifies the voltage sag at bus  $i$  (a  $PCC$ ) resulted from a fault at node  $j$ .  $z_{ij}$  refers to the impedance between  $PCC$  and fault location  $j$ .  $z_f$  and  $z_s$  represent the fault impedance and the source impedance at  $PCC$ .  $N$  and  $N_{PCC}$  are the number of buses and the length of  $PCC$ , respectively.

C) Total harmonic distortion (THD): THD is a criterion indicating the harmonic distortion level in a system. As it is presented in Equation 16, THD is defined as the summation of all harmonic components of a signal over the fundamental component [51].

$$F3 = \sum_{i=1}^{N_{pcc}} \frac{\sqrt{\sum_{h=2}^m |V_i^h|^2}}{|V_i^1|} \quad (16)$$

where,  $V_i^h$  is the voltage of bus  $i$  related to the harmonic  $h$ . And  $m$  denotes the number of harmonics to be considered.

The following three constraints need to be satisfied:

$$V^{\min} \leq V_n \leq V^{\max} \quad (17)$$

$$I_l \leq I_l^{\max} \quad (18)$$

$$\frac{|V_n^-|}{|V_n^+|} < UF^{\max} \quad (19)$$

Equation 17 represents voltage limits for different buses in the network. Equation 18 refers to feeder capacity limits for different branches. And Equation 19 considers the unbalance condition of distribution system where  $V_n^-$  and  $V_n^+$  stand for the negative and positive voltage sequences of bus  $n$ . And  $UF^{\max}$  indicates the maximum allowed unbalance factor. It is notable that the fourth constraint that should be checked for any configuration is its radiality which will be discussed in this chapter.

### 3.2 Fuzzy Pareto dominance algorithm

Although the single objective (SO) optimization approach (i.e. lumping all objectives into one objective) is more straightforward for solving optimization problems with several objectives, this approach is unable to identify alternative solutions. Pareto-dominance algorithm is a branch of evolutionary computation that provides a wider range of alternative solutions leading to more flexibility in the process of decision making and operation of the network.

Based on the basic definition of a Pareto-dominance model, solution  $x$  dominates  $y$  if and only if [52]:

$$f_i(x) \leq f_i(y) \quad \forall i \in \{1, 2, \dots, n\} \quad (20)$$

Based on Equation 20, a Pareto frontier will refer to a set whose members are not dominated by the other possible solutions (i.e.  $P = \{x : \{y \succ x\} = \emptyset\}$ ). Figure 10 illustrates how the solution  $y$  is dominated by solution  $x$  in an optimization problem with two objective functions. The members of optimal Pareto frontier indicating the non-dominated solutions are presented by solid circles.

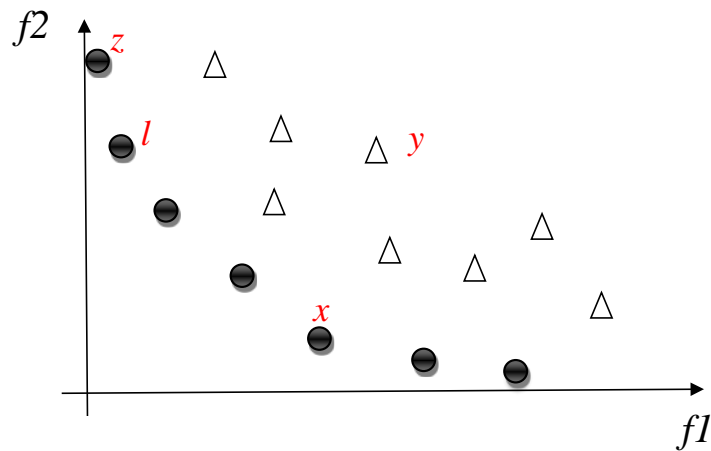


Figure 10: Pareto frontier identified by a typical Pareto-dominance algorithm

Different Pareto dominance algorithms have been proposed in the literature. In [53] improved strength Pareto evolutionary algorithm (SPEA) has been developed. In [40] a multi-objective evolutionary method called Pareto envelope-based selection algorithm (PESA) is introduced. In [54] Pareto archived evolution strategy (PAES) is proposed that uses archived previously identified answers to find the dominance ranking of the current and candidate solutions. In [46] a Niche Pareto based genetic algorithm (NPGA) is presented that degrades the fitness values of the "Elite Group" in each generation to identify the near-to-optimum solutions.

In this chapter, fuzzy Pareto dominance (FPD) technique is utilized to recognize the non-dominated network configurations identified by the global optimization algorithm. FPD assigns certain levels of dominance between each two solutions based on mutual fuzzy-based dominance degrees [53]. Therefore, FPD does not consider the solid circles in Figure 10 equally optimal. This is the major advantage of this technique over the conventional Pareto-dominance models.

According to FPD, vector (i.e. solution)  $a$  is dominated by vector  $b$  at the degree of  $\mu_p$  [53]:

$$\mu_p(a,b) = \frac{\prod_i \min(a_i, b_i)}{\prod_i b_i} \quad (21)$$

where,  $a$  and  $b$  indicate fitness values of the corresponding solutions. The degree of dominance varies between zero and one. If it equals to one,  $a$  is absolutely dominated by  $b$ . If  $\mu_p(a,b)$  and  $\mu_p(b,a)$  are both less than one, the vectors are non-dominated (e.g. the position of  $x$  and  $z$  in Figure 10). Although  $y$  is not absolutely dominated by  $z$ , it cannot be considered as a member of the optimal Pareto frontier since there is an  $l$  which has the same value of  $f_2$  but a lower value of  $f_1$  compared to  $y$ .

Finally, the average of  $\mu_p$  is assumed as the rank of  $a$ :

$$r_M(a) = \text{mean}_{b \in M} \{ \mu_p(a,b) \} \quad (22)$$

where,  $M$  represents all the possible answers.

The solution with the lowest value of  $r_M(.)$  stands for the most fertilized individual (i.e. configuration).

### 3.3 A reliability based network encoding

One important step in optimal network reconfiguration is encoding the topology of the network. In general, there are four major network (called “frog” in this chapter) coding techniques: 1) Vertex (i.e. node) based methods [40] in which the number of bits of each frog corresponds to the number of buses (i.e. nodes) in the network. This technique automatically creates radial configurations but it leads to large-size frogs for large systems containing many buses; 2) Branch based strategies [54] which automatically create radial frogs whose number of bits is proportional to the number of branches in the network; 3) Binary switch based approach which develops binary individuals (i.e. frogs) whose number of bits is the same as the number of switches in the system. This technique does not guarantee producing radial configurations and requires a tedious radial checking procedure to remove the infeasible frogs, 4) Loop (i.e. mesh) based algorithms [55] that automatically create radial frogs. The number of bits in each frog is equivalent to the number of meshes in the network.

As the number of loops in a system is noticeably less than the number of branches and



nodes, the loop-based strategy is computationally more efficient for encoding large distribution networks. In this chapter, this approach is adopted to encode the SFLA frogs. Therefore, the number of bits of each frog is equal to the number of loops in the network. Each bit indicates the branch number, located in the corresponding loop that should be open. For instance, the encoded frog for the network configuration shown in Figure 11 is  $F1 = \{10, 4\}$ . As long as there is no more than one open branch in each common feeder (in Figure 11 the common feeder refers to branches #5 and #6), the developed frog represents a radial configuration. As an example, any developed frog for the network presented in Figure 11 is radial except  $\{6, 6\}$ ,  $\{5, 5\}$ ,  $\{6, 5\}$  and  $\{5, 6\}$ . It is notable that the infeasible configurations should be automatically avoided which will be discussed in details in this chapter.

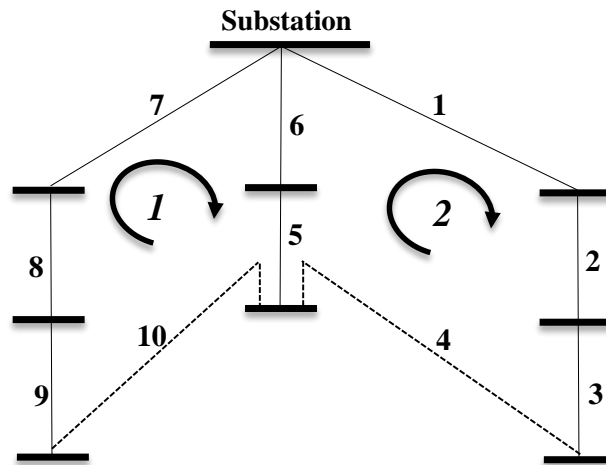


Figure 11: A radial network with two loops

It is desirable that the aged and risky switches less participate in the reconfiguration procedure. To address this issue, in this chapter, a systematic approach is proposed to be used in the encoding stage of the initial population. By adopting this initialization technique, the

optimization process identifies the suboptimal configurations with a less risky switching number.

Two fuzzy values, between zero and one, are assigned to each switch (it is assumed there is one switch installed at each branch). The output of the first fuzzy function depends on the age of the associated switch. Since older switches are less desired to participate in the process of reconfiguration, less values of  $g1$  (refer to Figure 12) will be assigned to the aged switches. For instance, if switch #9 is older than switch #3 in Figure 11, the first function returns a higher value of  $g1$  for the latter. The second fuzzy function returns a value of  $g2$  (refer to Figure 12) that corresponds to the “distance” of the relevant switch from the closest critical branch. If it is assumed that the critical branches in Figure 11 are the branch #1, #6 and #7 (because they are closer to the substation bus), the distance vector for the ten branches in the network is {0, 1, 2, 2, 1, 0, 0, 1, 2, 2}. For simplicity, the branches are assumed to have an equal length. As it can be seen, the branches #3, #4, #9 and #10 have the longest distance from the relevant closest critical branch. Therefore, these four branches allocate a higher value of  $g2$  to themselves and they will be more desired to participate in the process of the reconfiguration as the malfunction of switch #3 or #9 only affects one bus while the failure of switch #2 affects two buses.

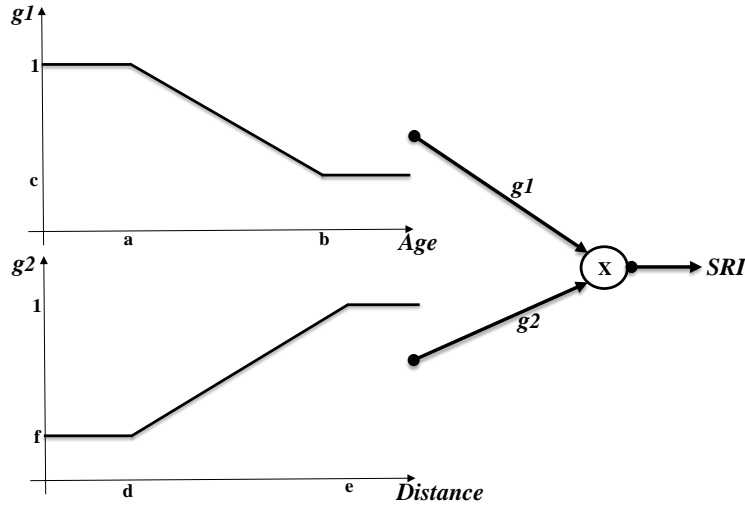


Figure 12: The fuzzy functions calculating SRI for each switch

Finally, according to Figure 12, the switch reliability index (SRI) is calculated for each switch which is equal to the multiplication of  $g1$  and  $g2$ . SRI will then be incorporated in the roulette-wheel selection process [46] that is adopted to systematically select one switch per loop to participate in the optimization procedure. For example, if the vector of SRI for branch #1-6, located in the second loop of the network in Figure 11, is  $\{0.2, 0.7, 0.95, 0.85, 0.75, 0.35\}$ , the chance of switch #3 to be selected as the second bit of the initial frog is the highest.

### 3.4 Shuffled frog leaping algorithm with adaptive local search

Shuffled frog leaping algorithm (SFLA) is a meta-heuristic search method inspired by the memetic evolution of a group of frogs looking for food [56]. Based on the concept of memetic evolution, SFLA considers the possibility of infection of ideas from one individual to another

one in a local search area. A shuffling methodology is also permitted to make this algorithm able for the exchange of information between local searches in order to yield a global optimum. This algorithm combines a deterministic and random approach. The deterministic strategy forces the method to use response surface information in order to guide the heuristic search as effective as possible. However, the random elements result in a more robust and flexible search pattern.

In the rest of this section, at first, the concept of SFLA is briefly explained. Then, the shortcoming of this global optimization algorithm for being applied to the network reconfiguration problem is discussed. Finally, a systematic approach is proposed to address this caveat.

Suppose there are several stones and a group of frogs in a swamp. The main goal of the frogs is to find the stone with the maximum food. The frogs have the permission to communicate with each other to improve their memes. Meme improvement is achieved by changing leaping steps of each frog so that an individual frog's position becomes closer to the best stone.

The first step to simulate SFLA is to randomly generate a certain number of feasible frogs as the initial population. At a later stage, the frogs are sorted in a descending order based on their fitness values. Then, all of the frogs are divided into  $m$  memplexes, each of which contains  $n$  frogs. In order to classify the frogs, the first member of the sorted set is put in the first memplex, the second one in the second memplex, the  $m$ th one in the  $m$ th memplex, the  $(m+1)$ th one in the first memplex and so on. By partitioning the frogs, a set of “parallel frog cultures” are created which try to move towards the main goal individually in parallel.

At the next stage, an evolutionary method is applied to the worst frog (the one with the worst fitness value) in each memplex to improve its position (i.e. to become closer to the stone

containing the maximum food). The following equations show this process that is called “local search”:

$$D = rand().(X_b - X_{w,old}) \quad (23)$$

$$\begin{aligned} X_{w,new} &= X_{w,old} + D; \\ -D_{max} &\leq D \leq D_{max} \end{aligned} \quad (24)$$

where,  $rand()$  is a random number between zero and one.  $X_b$ ,  $X_{w,old}$  and  $X_{w,new}$  refer to the best frog, the current worst frog and the new frog in the corresponding memeplex, respectively.  $D$  and  $D_{max}$  stand for the step size and the maximum allowed step size. If this strategy generates a better frog with a lower fitness value, the new frog replaces the old one. Otherwise, the same process should be repeated with a difference that instead of using the local best frog in Equation 23 the global best frog (i.e. the best frog in all memeplexes) should be used. If using the global best frog does not improve the worst frog either, a new frog is generated randomly that replaces the worst one. Finally, the entire individuals in different memeplexes are combined and all the steps are repeated until a convergence criterion is satisfied. The final step, that is called shuffling process, improves the meme quality and makes the cultural evolution free from any bias. In this step, all the frogs in different memeplexes are combined together to build a united population. More details about the implementation of SFLA can be found in [23].

The above mentioned SFLA procedure is not directly applicable to the distribution network reconfiguration task since it does not guarantee the feasibility and radiality of the

generated frogs through the local search step. In other words, some generated frogs (i.e. distribution system configurations) via Equations 23 and 24 might be: (1) infeasible; which means the generated frog may contain bits that refer to the switches not existing in the corresponding loop. For example, the created frog for Figure 11 is not feasible if its first bit refers to a branch number that is located in loop #2, (2) non-radial; for example, the frog {5, 6} generated for Figure 11 is not radial.

The most straightforward strategy to address this challenge is to repeat the local search procedure for each memplex and iteration of SFLA until feasible and radial (F&R) configurations are identified. Despite of its simplicity, this process is too time-consuming for large distribution networks and it significantly increases the computation burden of the algorithm. Another possible simple technique to solve this problem is to assign a penalty factor to the objective functions (refer to Equations. 2-3 and 15-16) for generated non-F&R frogs. Applying this method still reduces the convergence speed since the optimization algorithm needs to be executed for more iterations to learn the consequence of generating non-F&R configurations (i.e. with higher objective values).

In this chapter a novel "adaptive local search" is proposed that automatically generates F&R frogs in the local search step of SFLA which significantly reduces the computation burden of the algorithm. In the proposed method a matrix called Loop-Branch Cell-Matrix (LBCM) is introduced whose dimensions is  $L \times L$ , where  $L$  represents the number of loops in the network. Each element of LBCM contains a vector called Cell Vector (CV). The CVs located on the diagonal components of LBCM contain the branch numbers of the corresponding loops. However, the CVs related to the non-diagonal components of LBCM consist of the common

branches between the relevant loops. The procedure to implement the proposed technique is as follows:

- 1) *Implement Equations 23 and 24 to calculate  $X_{w,new}$ .*
- 2) *Repeat this process for  $l=1:L$ .*
- 3) *If the loop number ( $l$ ) is more than one, go to 4. Otherwise, go to 5.*
- 4) *for  $m=1:l-1$ ; if any component of  $LBCM(l,m)$  has been selected so far,  $LBCM(l,l)=LBCM(l,l)-LBCM(l,m)$ .*
- 5) *Round  $X_{w,new}(l)$  to the closest component of  $LBCM(l,l)$ .*

Once the LBCM is created, it is used to modify the output of local search of SFLA so that any possible non-F&R configuration will be converted into an F&R configuration, which significantly increases the speed of the optimization process.

Considering Figure 13 as an example, the LBCM has four rows and four columns. It is assumed that the best and the worst configurations of Figure 13 are {10, 4, 16, 11} and {7, 2, 18, 10}, respectively. Applying Equations 23 and 24 to these frogs, the vector of  $X_{w,new}$  will be obtained. According to Equation 25, the first generated bit of the frog is 9.6 that should be rounded to the closest integer value corresponding to  $LBCM(1,1)$ , which is  $CV=\{5,6,7,8,9,10\}$ . Therefore, the first modified bit becomes "10". The second bit is 2.9. The CVs of  $LBCM(2,2)$  and  $LBCM(2,1)$  are {1,2,3,4,5,6} and {5,6}, respectively. Since any element of  $LBCM(2,1)$  has not been selected yet,  $LBCM(2,2)$  remains unchanged and 2.9 is rounded to "3".

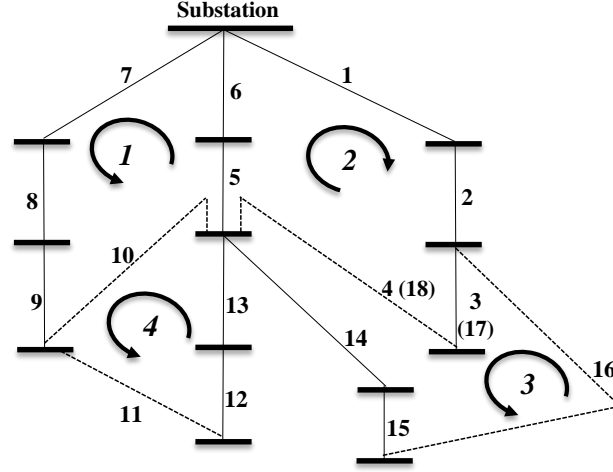


Figure 13: The sample network used to clarify the adaptive local search step

$$X_{w,new} = \begin{bmatrix} 7 \\ 2 \\ 18 \\ 10 \end{bmatrix}^T + rand(1,4) \times \begin{bmatrix} 10-7 \\ 4-2 \\ 16-18 \\ 11-10 \end{bmatrix}^T = \begin{bmatrix} 9.6 \\ 2.9 \\ 17.7 \\ 10.3 \end{bmatrix}^T \quad (25)$$

The third bit is 17.7. The CVs of LBCM(3,3), LBCM(3,1) and LBCM(3,2) are {14,15,16,17,18}, { $\emptyset$ } and {17 (3), 18 (4)}, respectively. Since the branch #3 has been already picked, LBCM(3,3) is changed into {14,15,16}. Therefore, 17.7 is rounded to "16". Finally, the fourth bit is 10.3. The CVs of LBCM(4,4), LBCM(4,1), LBCM(4,2) and LBCM(4,3) are {10,11,12,13}, {10}, { $\emptyset$ } and { $\emptyset$ }, respectively. Therefore, LBCM(4,4) should be changed into {11,12,13} because the branch #10 was selected for the first loop. As a result, 10.3 is rounded to "11" to create the new frog of {10, 3, 16, 11} as the output of the adaptive local search step.

It is notable that according to Equation 25 the output of the conventional local search of SFLA is {10, 3, 18, 10} which is obviously non-radial. However, as explained above, the output



of the proposed adaptive local search is F&R.

### 3.5 Implementation

The pseudo code of the proposed fuzzy Pareto dominance adaptive shuffled frog leaping algorithm (FPD-ASFLA) for identifying a Pareto frontier as the high-quality suboptimal network configurations is as follows:

- 1) *Generate the initial population of frogs using the reliability based systematic encoding proposed in 3.3.*
- 2) *Put Iteration=1.*
- 3) *Run Newton–Raphson power flow program.*
- 4) *Calculate power loss, voltage sag and THD for each frog using Equations 2-3 & 15-16.*
- 5) *Compute the rank of each frog using Equations 21 and 22.*
- 6) *Sort the individuals in a descending order based of their rank.*
- 7) *If Iteration >1 go to 8, directly. Otherwise, save the best frog (i.e. the configuration with the lowest rank) in the archive set (AS)) and go to 10.*
- 8) *Calculate the domination degree of each frog in population proportional to all the frogs in AS, using Equation 21. If there is no frog in AS dominating the relevant individual in the population, it will be added to AS as a new member. This process will be repeated for all the frogs in population.*

9) Compute the domination degree of each old member in AS proportional to all the new members of AS. If there is even one new member dominating the relevant old frog, the old individual will be removed from AS. This process will be repeated for all the old members of AS.

10) Sort and partition all the frogs in  $m$  memeplexes based on the method presented in 3.4.

11) Repeat the process of local search (LS) for each  $m$  memeplex, using Equations 11 and 12, until  $LS\_Iteration = Max\_LS\_Iteration$ . And modify the topology of each recently created frog in this step through the presented strategy in 3.4 to develop F&R individuals.

12) Apply the shuffling process, as it was explained in 3.4, to combine all the frogs in different memeplexes and create a united population.

13) If  $Iteration = Max\_Iteration$ , go to 14. Otherwise,  $Iteration = Iteration + 1$  and go to 3.

14) Report all the frogs saved in the most recently AS as the suboptimal network configurations identified by the proposed hybrid optimization algorithm. Based on the network operational situation, the operator will decide to rely on which configuration of the optimal Pareto frontier.

### 3.6 Simulation results and discussions

The proposed algorithm is implemented in MATLAB software on a computer with the processor of Intel(R) Xeon(R) CPU E5-2603 0 @ 1.80 GHz. The performance of the proposed hybrid FPD-ASFLA algorithm is demonstrated by its implementation on a 136-bus distribution network [57], that is shown in Figure 14. The tie switches are distinguished by dash lines and red numbers. This network contains 156 branches and 21 loops. It is assumed that one switch is installed at each branch. It is notable that adopting the loop-based encoding strategy leads to frogs with only 21 bits, which significantly reduces the computational burden of the optimization algorithm compared to the case of branch-based or node-based coding techniques.

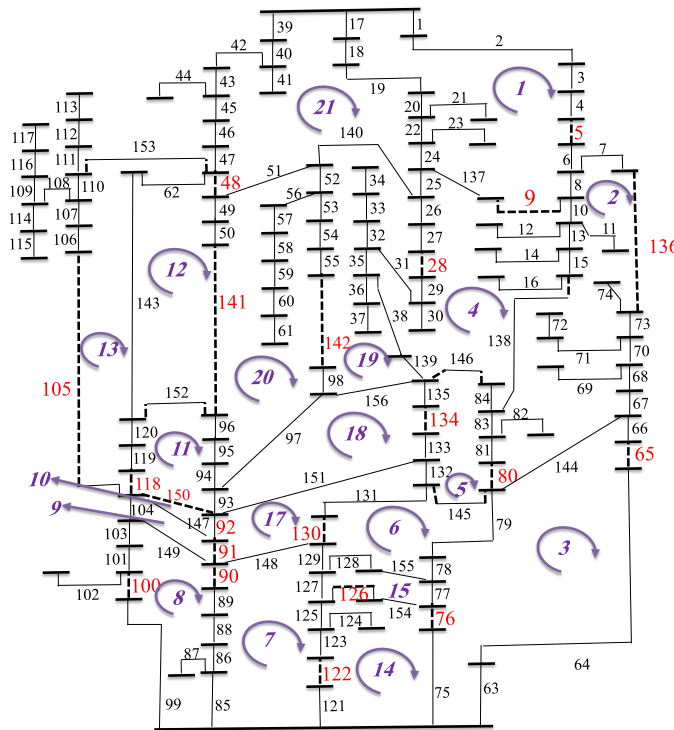


Figure 14: A 136-bus distribution network with 21 loops (Loop #16 contains branch numbers {1-7, 136, 73, 70, 63-68, 99-101, 103-107, 110, 153, 45-47, 43, 42, 40, 39}) [57]

The calculated  $g1$ ,  $g2$ , and  $SRI$  values (according to section 3.3) for all the switches are presented in Figure 15. For simplicity, the length of all branches is considered to be equal. As it can be observed, the probability of selecting switch #9 for encoding the initial frogs is much higher than an aged switch (e.g. #8) or a switch with a more critical location (e.g. #17).

To consider nonlinear loads for the network, 19 harmonic currents as the percentage of fundamental currents are defined for 11 buses of the system which are presented in Table 3. Also, four points of common coupling are assumed for Bus #12, 20, 24 and 28.

Table 3: Nonlinear Load Data (Percentage of Fundamental Frequency)

<b>Bus No.</b>	<b>Harmonic No.</b>								
	<b>3</b>	<b>5</b>	<b>7</b>	<b>9</b>	<b>11</b>	<b>13</b>	<b>15</b>	<b>17</b>	<b>19</b>
<b>7</b>	0	30	0	0	8	6.8	0	4.1	3.2
<b>8</b>	90	60	45	28	10	8	6	5	4
<b>11</b>	75	56	34	6	13	0	0	0	0
<b>16</b>	0	1	1	0	8	4	0	0.2	0.1
<b>21</b>	0	90	85	0	65	0	0	34	5
<b>26</b>	0	95	90	0	70	65	0	46	10
<b>45</b>	0	40	20	0	9	7.7	0	0.7	0.4
<b>52</b>	80	53	31	13	7	5.5	5	4.5	1.1
<b>54</b>	0	2	2	0	9	5	0	0.3	0.2
<b>63</b>	0	50	30	0	10	8.9	0	6.2	4.3
<b>91</b>	85	65	40	8	33	36	0	0	0

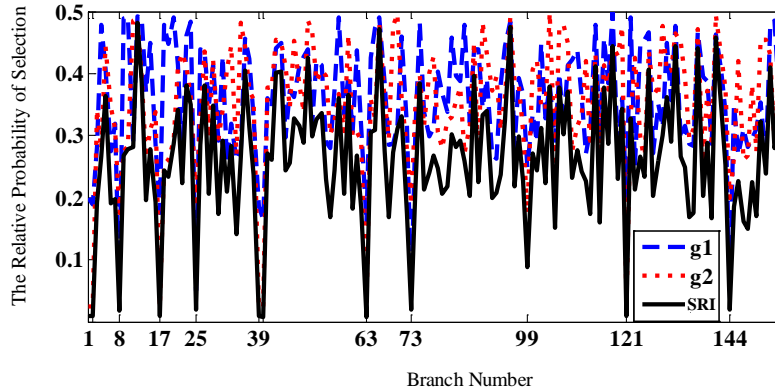


Figure 15: The determined SRI of each switch

The algorithm stops when it reaches Iteration #100 after repeating the local search process 10 times for each iteration (i.e. LS\_Iteration=10). The performance of the proposed algorithm (FPD-ASFLA) is compared with FPD-SFLA (i.e. the proposed hybrid model without adapting the local search step) and FPD-GA (i.e. applying the same Pareto dominance technique to genetic algorithm). In order to provide a fair comparison, these three optimization algorithms start the searching process from the same initial frog population.

The growing trend of the number of *archive set (AS)* members during the optimization procedure is shown in Figure 16. The minor reductions observed in this figure are due to applying *step 9* in 3.5. As it can be inferred, FPD-ASFLA, FPD-SFLA and FPD-GA will identify 31, 55 and 26 non-dominated frogs in their AS after 100 iterations.

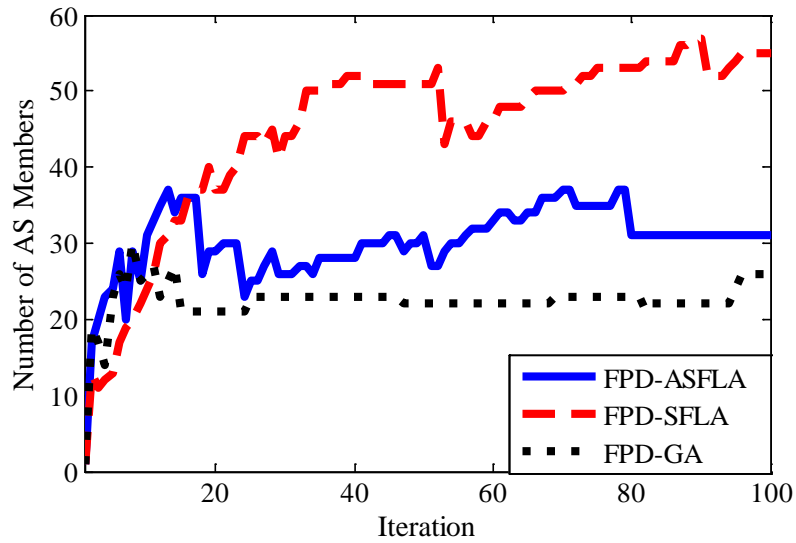


Figure 16: The number of AS members

Since a number of non-dominated solutions with three fitness values (i.e. power loss, voltage sag and THD) are identified in each iteration, the average fitness value of the updated AS members is selected to present the progress of algorithm. The declining trend of average fitness values for the three algorithms is depicted in Figure 17. Comparing Figures 16 and 17, it can be realized that although FPD-SFLA has identified a higher number of non-dominated frogs, FPD-ASFLA provides the higher qualified suboptimal solutions.

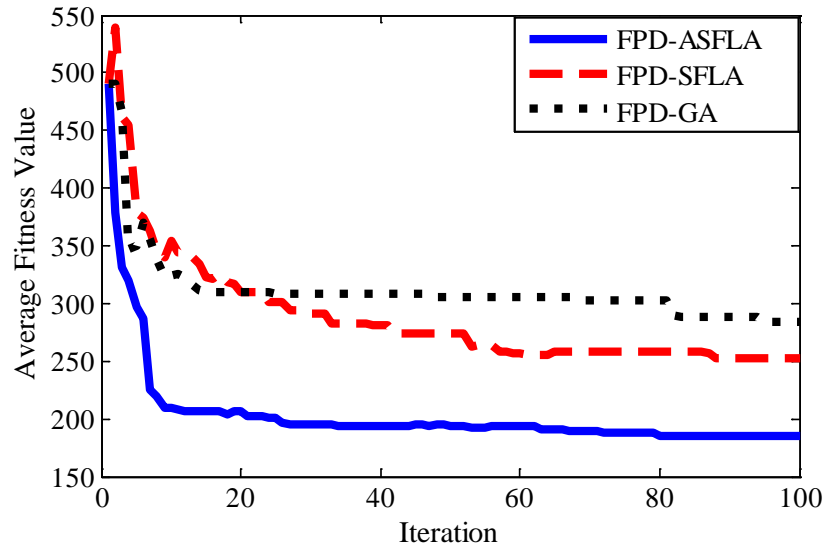


Figure 17: The declining trend of average fitness values

Table 4 provides a more detailed comparison between the performance of the mentioned algorithms and the corresponding single models (i.e. single objective SFLA and GA). As it can be noticed, the computational burden of FPD-ASFLA is considerably less than that of the Pareto based models; however, single objective SFLA has the lowest operation time. On the other hand, FPD-ASFLA has identified the configurations with the lowest power loss, voltage sag and THD on its Pareto frontier.

Table 4: Performance of Different Algorithms

Algorithm	<i>Min Power Loss (KW)</i>	<i>Min Voltage Sag</i>	<i>Min THD</i>	<i>Computational Burden (S)</i>
FPD-ASFLA	<b>302.3581</b>	<b>133.5097</b>	<b>9.0130</b>	40225
FPD-SFLA	359.7075	133.7960	9.1486	56803
FPD-GA	383.1015	133.8021	9.2734	61235
SFLA	448.2174	134.1437	9.2704	<b>31592</b>
GA	512.3001	134.4138	9.0475	36406
Initial Topology	3950.7010	134.6190	16.4017	-

The declining trend of fitness values recognized by FPD-ASFLA over the optimization process is illustrated in Figure 18. Figure 18 (a) shows the average fitness values of all the frogs in AS. By comparing Figures 16 and 18 (a) it can be noticed that the average of fitness values gradually decreases while the number of AS members increases at the same time. This observation verifies that the new fertilized solutions identified by the algorithm are improving the quality of AS. Similarly, Figures 18 (b-d) depict the general declining trend of power loss, voltage sag and THD as the algorithm proceeds. Due to the nature of a Pareto based optimization model, there is no necessity for the algorithm to reduce all the fitness values in each iteration since the main goal is identifying non-dominated solutions. This fact can be observed in Figure 18.



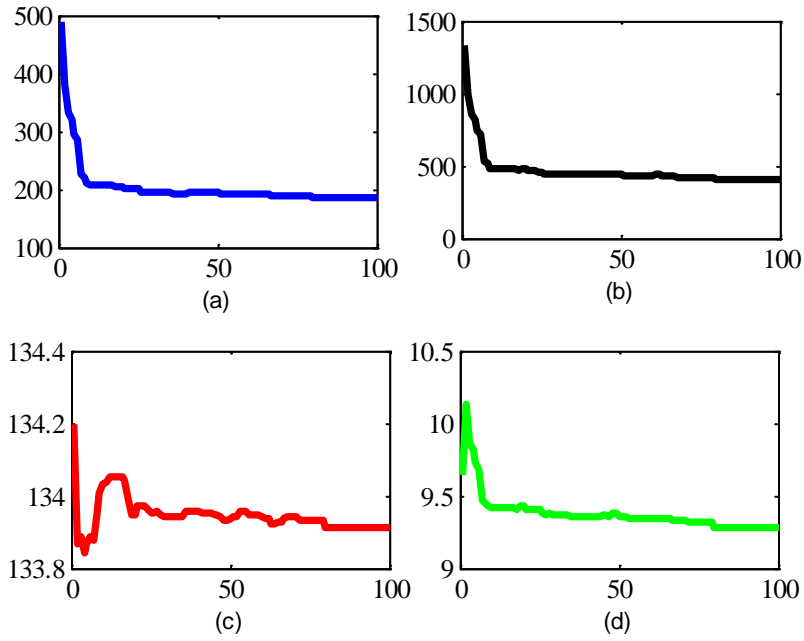


Figure 18: The declining trend of fitness values ((a): average; (b): power loss; (c) voltage sag; (d) THD)

Among  $2^{156}$  possible configurations for the network, the proposed algorithm finds 31 non-dominated solutions on the Pareto frontier which is shown in Figure 19.

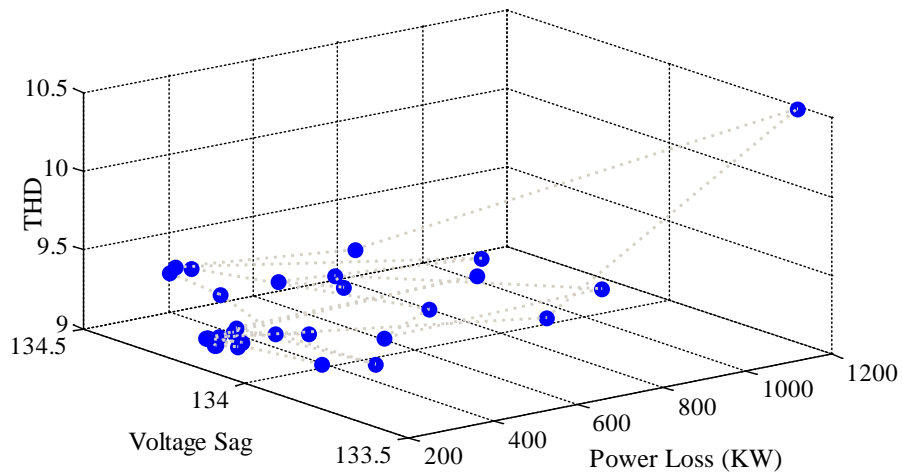


Figure 19: The identified Pareto frontier

Once the optimal Pareto frontier is identified, among the 31 candidates, the most appropriate configurations can be selected based on the operator's decision. For instance, four scenarios are defined in this section as follows: (1) a configuration is desired that causes minimum power loss; (2) a configuration is desired that causes the minimum voltage sag; (3) a configuration is desired that causes the minimum THD; (4) a configuration is desired that causes the minimum average of power loss, voltage sag and THD. The suboptimal frogs for the defined scenarios will be: (1) {9, 83, 79, 84, 135, 145, 148, 90, 104, 150, 120, 141, 106, 126, 128, 7, 92, 98, 139, 96, 51}; (2) {8, 67, 78, 15, 135, 145, 148, 90, 147, 150, 118, 141, 110, 123, 154, 47, 92, 151, 139, 142, 48}; (3) {9, 15, 79, 84, 135, 145, 148, 90, 104, 150, 119, 141, 106, 126, 128, 7, 92, 98, 139, 96, 51}; (4) {9, 83, 79, 84, 135, 145, 148, 90, 104, 150, 119, 141, 106, 126, 128, 7, 92, 98, 139, 96, 51}.

Table 5 compares the impact of conventional and the proposed reliability based encoding approaches on the quality of the identified Pareto frontier. According to this table, if the proposed encoding method is used, the number of risky switching that is scheduled in the suboptimal configurations significantly reduces. It is notable that, in Table 5, the change in the status of a given switch is considered as a risky operation if the associated *SRI* for the switch is less than 0.2.

Table 5: The Effect of the Proposed Reliability-based Encoding Strategy on the Performance of the Algorithm

	Power Loss (KW)	Voltage Sag	THD	High Risky Operations
<i>Proposed Encoding</i>	432.85	134.09	9.28	<b>9</b>
<i>Conventional Encoding</i>	430.07	134.83	9.65	<b>34</b>

### 3.7 Summary

In this chapter, a novel hybrid optimization algorithm based on the combination of fuzzy Pareto dominance (FPD) and shuffled frog leaping algorithm (SFLA) is proposed to solve the multi-objective optimization problem of distribution network reconfiguration with the purpose of minimizing power loss, voltage sag and THD. It identifies a Pareto frontier as the non-dominated suboptimal configurations. The local search step of SFLA is customized for the application of power system reconfiguration that significantly reduces the computational burden of the algorithm. A reliability based encoding strategy is also developed that selects more reliable solutions as the start point of the optimization procedure. The performance of the proposed hybrid optimization algorithm is demonstrated by its implementation on a 136-bus distribution network. The simulation results verify that the proposed optimization algorithm not only is much faster in convergence compared to the similar Pareto based models but also it identifies more fertilized solutions. It is also demonstrated that the proposed reliability based initial encoding leads to more reliable solutions found by the algorithm after 100 iterations.

# CHAPTER FOUR: OPTIMAL DISTRIBUTION NETWORK RECONFIGURATION USING DYNAMIC FUZZY BASED GENETIC ALGORITHM

## 4.1 Overview of genetic algorithm

The three main optimization tools employed in engineering problems are neural networks (NNs), machine learning and evolutionary computation (EC). GA is known as the most prominent and popular member of EC family. GA performs based on the idea of natural selection to evolve a population of chromosomes as the candidate solutions to a given problem using its operators that are selection, crossover, and mutation. According to the principle of "survival of the fittest", the first operator selects the chromosomes based on their fitness values to participate in the reproduction of the next generation. The second operator changes subparts of each two chromosomes, selected by the first operator, to produce two new individuals. In order to maintain the genetic diversity of a population, mutation is utilized to alter one or more gene values of each chromosome that produces a new individual for the next generation. More details about the concept of GA and its implementation can be found in [58]. The procedure of solving the reconfiguration optimization problem by GA is explained as follows:

*Step 1) Generate  $N$  chromosomes randomly as an initial population.*

*Step 2) Run the load flow program.*

*Step 3) Compute the fitness value of each individual.*

*Step 4) Select  $N$  chromosomes based on the adopted selection strategy.*

*Step 5) For each two selected chromosomes, generate a value between zero and one, randomly. If this value is less than the crossover probability, apply the adopted crossover strategy to the pair to create two new chromosomes which replace the two old ones. Otherwise, the pair remains unmodified.*

*Step 6) For each chromosome, generate a value between zero and one, randomly. If this value is less than the mutation probability, apply the mutation strategy on the chromosome to produce a new individual. Otherwise, the chromosome is directly transferred to the next step without any change.*

*Step 7) If the stopping criterion is satisfied, print the chromosome with the minimum fitness value as the final solution and go to step 8. Otherwise, go to step 2.*

*Step 8) Finish.*

#### 4.2 Determining crossover and mutation parameters

The crossover and mutation parameters, which are presented as  $P_c$  and  $P_m$ , respectively, indicate the probabilities based on which crossover and mutation occurs. The efficient performance of GA critically originates from a successful crossover and mutation. Therefore, an accurate technique to determine  $P_m$  and  $P_c$  plays a significant and undeniable role in the behavior of GA [59]. The value of  $P_c$  controls the speed of exploiting process in identifying the best answer in a local area. On the other hand, the value of  $P_m$  adjusts the speed of algorithm in exploring new regions. Therefore, a meaningful relationship between crossover and mutation

probabilities is necessary to prevent the algorithm from falling into local optimums, which is the result of a weak exploration, or from having a low convergence speed, that is the consequence of a poor exploitation.

Conventionally, trial and error procedures were used by researchers to find fixed values for  $P_c$  and  $P_m$ . For instance, trial and error experiments are utilized in [60] to determine the fixed  $P_c$  and  $P_m$  values of a GA that is employed to tune the node connection weights of an artificial neural network (ANN) in load forecasting. Despite of their simplicity, there is a main disadvantage accompanied with these trial and error techniques. As the algorithm proceeds, the optimal contribution rates of crossover and mutation varies that brings about the necessity of having different crossover and mutation probabilities for different chromosomes and different generations [61]. However, these trial and error methods can provide only one single  $P_c$  and  $P_m$  for all the chromosomes in different generations. For this reason, a self-adaptive GA is proposed in this chapter, which is able to automate the parameters setting process and update them dynamically as the evolution of chromosomes goes forward.

In this chapter, the concept of fuzzy membership functions is utilized to introduce a dynamic strategy for determining  $P_c$  and  $P_m$ . The process is elaborated in this section for the mutation operator. The first function,  $f_l$ , assigns a fuzzy membership value between zero and one, shown as  $p_1$ , to the chromosome based on the distance of its fitness value from the best fitness value in the same generation. If the chromosome is close to the best individual,  $f_l$  assigns a lower value to the chromosome to decrease the probability of mutation and increase the survival possibility of that chromosome in the next generation. On the other hand, if the chromosome is far from the best individual,  $f_l$  assigns a higher value to the chromosome to

increase the mutation probability with the hope of producing a new chromosome with a better fitness value. The first fuzzy function is depicted in Figure 20.

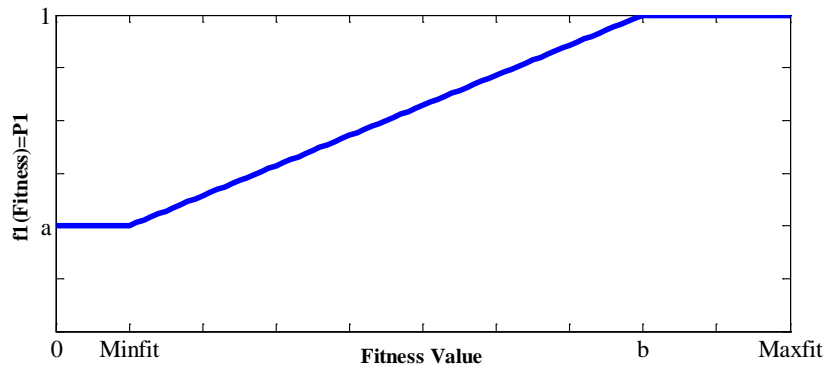


Figure 20: The fuzzy function determining P1

The second function,  $f2$ , assigns a fuzzy value, shown as  $p_2$ , to the chromosome based on the distance of the average fitness value of all the chromosomes in the same generation from the best fitness value. It is notable that the calculated fuzzy membership value is equal for all the chromosomes in the same generation. If the average fitness value is close to the best individual's fitness, it means all the chromosomes in the population are converging to one individual which increases the risk of falling into a local optimum. As a result,  $f2$  assigns a higher value to all the chromosomes to raise the mutation probability and explore new regions. On the other hand, if the average fitness value is far from the best fitness value, it means the chromosomes are exploring too much and they do not consider the existing optimum in their locality. For this reason,  $f2$  determines a lower value for  $p_2$  to decrease the mutation probability and gain up the speed of exploiting process. The second fuzzy function is illustrated in Figure 21.

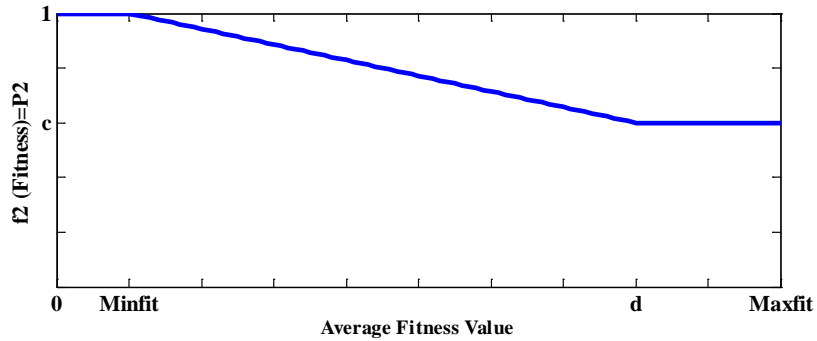


Figure 21: The fuzzy function determining P2

The third function,  $f_3$ , assigns a fuzzy value, shown as  $p_3$ , to each chromosome based on its age. If the chromosome has been just generated and it is young,  $f_3$  considers a lower value for  $p_3$  to decrease the mutation probability and increase the survival chance of the young chromosome to have more time to live and show its potential values. If the chromosome is middle-age, it has had enough time to exploit and it is time for  $f_3$  to assign a higher value to this chromosome and increase the probability of mutation to create a new child. Finally, if the chromosome is old, it means that the individual has been fertilized enough to survive in the different generations so far and the final global answer might be even close to this individual. Therefore,  $f_3$  decreases the  $p_3$  for this old chromosome to diminish the mutation probability and protect this individual from dying and being replaced by a new chromosome. The third fuzzy membership function is shown in Figure 22.



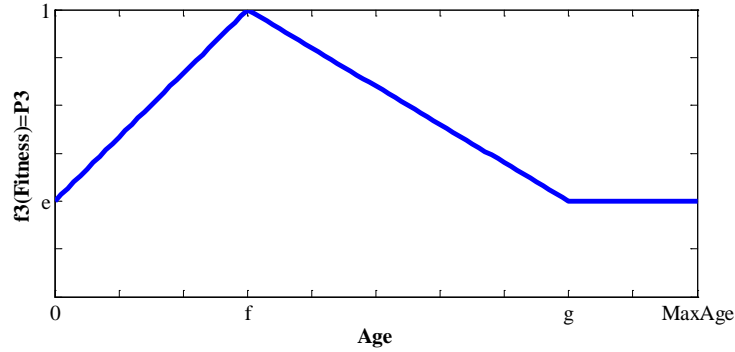


Figure 22: The fuzzy function determining P3

Therefore, the probability of mutation for each chromosome is calculated as follows:

$$P_m = P_{constant} \times P_1 \times P_2 \times P_3 \quad (26)$$

where, in Figures 20-22 and Equation 26 the fixed values of  $a$ ,  $b$ ,  $c$ ,  $d$ ,  $e$ ,  $f$ ,  $g$  and  $P_{constant}$  are determined through a trial and error procedure. The same process can be repeated for the crossover operator with only one difference that the x-axis in Figure 20 and 22 will stand for the average fitness and the average age of the corresponding pair, respectively.

#### 4.3 Simulation results and discussions

The presented method is developed in MATLAB and the simulation process is done on a computer with the processor of Intel(R) Xeon(R) CPU E5-2603 0 @ 1.80 GHz. The algorithm is

tested on a 33-bus radial distribution network [62] that is shown in Figure 23. It contains 32 sectionalizing switches and five tie lines.

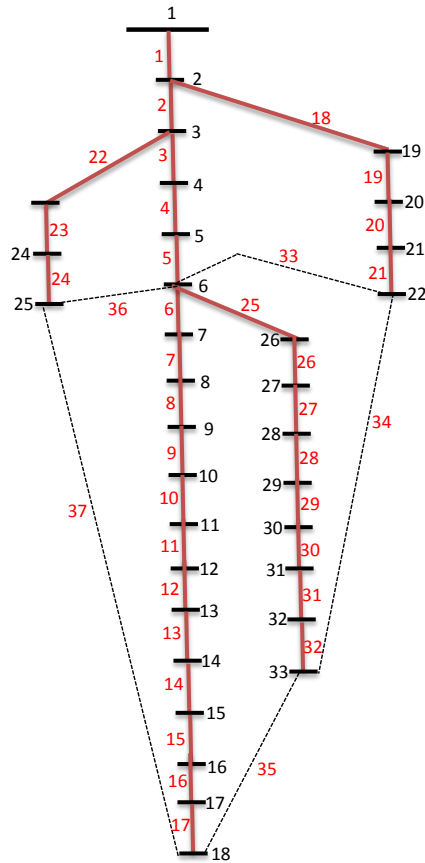


Figure 23: Case study [62]

The chromosome encoding strategy adopted in this chapter is the same loop-based encoding method elaborated in Chapter 3. The utilized coding technique is much faster and more computationally efficient than the branch-based and node-based strategies which would bring about the chromosomes with 37 and 33 genes, which are the number of branches and nodes, respectively. For instance, the generated chromosome  $Ch=\{33, 34, 35, 36, 37\}$  represents the

initial configuration (see Figure 23) in which all the branches are closed except the lines 33, 34, 35, 36 and 37. As can be inferred, the generated individual refers to a radial network since each of the five open branches corresponds to one separate loop number. Utilizing the loop-based encoding technique, GA is employed to randomly create  $N$  initial chromosomes signifying  $N$  radial networks.  $N$  is the number of population that is assumed to be 100 in the simulation. Then, load flow is run to compute the fitness value, which is the total power loss, for each configuration. At a later stage, the roulette wheel selection strategy [58] is adopted to select the more fertilized chromosomes with lower fitness values (i.e. lower total power losses). However, the less qualified individuals still have a low chance to participate in the next generation and increase the diversity.

Afterwards, the two point crossover technique is applied on the selected individuals. Adopting this method, a value is selected randomly between zero and one for each two chromosomes. If the random value is higher than the crossover probability, the two individuals survive and will transfer to the next step without any modification. Otherwise, two points are chosen randomly for each two chromosomes and the relevant genes between those two points are exchanged between the two individuals to produce two new children. And the generated children take part in the next step instead of their parents. Then, the chromosomes are mutated to guarantee a diverse population. For this purpose, a random value between zero and one is selected for each individual. If the value is less than the mutation probability, one of the genes of the chromosome is selected and its value will change. Since the non-radial configurations are not desirable, another branch from the same loop is randomly selected to replace the chosen gene. For instance, if the gene 33 (i.e. Branch #33) in  $Ch$  is chosen to be mutated, one of the branches

existing in the same loop (i.e. Branch #18, 19, 20, 21, 5, 4, 3 or 2) will replace it. Using this strategy, the radiality of distribution system after applying crossover and mutation is guaranteed and there is no need to go through the tedious radiality checking process after each iteration. It is notable if the conventional binary branch-based encoding strategy was used, not only each individual would contain 37 genes instead of only five bits, but also radiality checking would be necessary after each iteration that would increase the computation burden of the algorithm. As it was elaborated in 4.2, three fuzzy functions, shown in Figures 20-22, are used to dynamically tune the probability of crossover and mutation and control the behavior of GA during the time. These fuzzy functions are formulated as follows.

$$P_1(x) = \begin{cases} a & \text{if } x < m \\ \frac{(1-a) \times (x-m)}{b-m} + a & \text{if } m \leq x < b \\ 1 & \text{otherwise} \end{cases} \quad (27)$$

$$P_2(y) = \begin{cases} 1 & \text{if } y < m \\ \frac{(c-1) \times (y-m)}{d-m} + 1 & \text{if } m \leq y < d \\ c & \text{otherwise} \end{cases} \quad (28)$$

$$P_3(z) = \begin{cases} ((1-e)z/f) + e & \text{if } 0 \leq z < f \\ ((e-1)(z-f)/(g-f)) + 1 & \text{if } f \leq z < g \\ e & \text{otherwise} \end{cases} \quad (29)$$

where,  $m$  stands for the minimum fitness value corresponding to the best chromosome in each iteration. And  $a, b, c, d, e, f$  and  $g$  are the fuzzy functions' constant values that are determined through a trial and error procedure. After applying the trial and error technique, the following values are obtained for crossover and mutation.

$$Crossover : \begin{cases} a = 0.9; & c = 0.8; & e = 0.95; \\ & b = 5m; & d = 5m; \\ f = 4; & g = 12; & P_{constant} = 0.95 \end{cases} \quad (30)$$

$$Mutation : \begin{cases} a = 0.85; & c = 0.75; & e = 0.95; \\ & b = 6m; & d = 4m; \\ f = 4; & g = 12; & P_{constant} = 0.1 \end{cases} \quad (31)$$

Running the algorithm for 100 iterations, the best identified solution stands for a network with the power loss of 28.968 kW. The declining trend of the best fitness value in different iterations is shown in Figure 24. As it can be observed, the best solution has not been modified after the generation of 78.

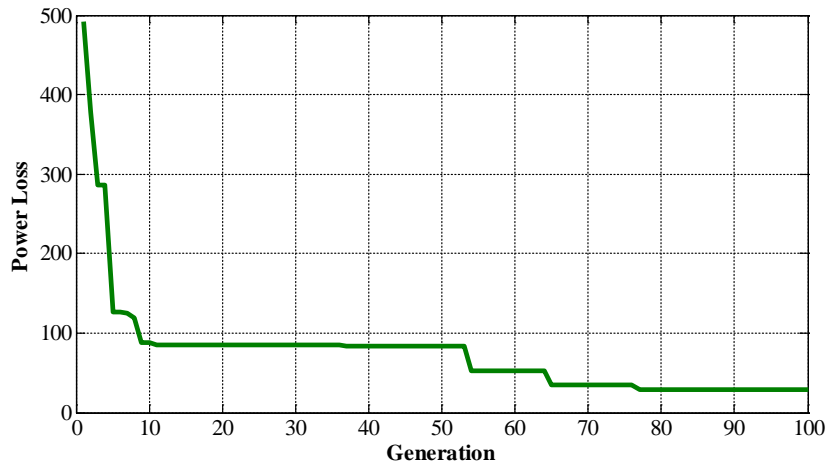


Figure 24: The trend of the best fitness value in each generation

In order to have an idea about the situation of the other chromosomes in each iteration, the alterations of the average and the best fitness values in different generations are illustrated in Figure 25. It can be vividly noticed that the other chromosomes try to update their situation based on the improvements of each generation's best individual. Although a considerable spark occurs at Iteration #88, which means that the created chromosomes in the 88th generation are not fertilized, the algorithm shows its robustness and rapidly modifies the poor qualified population by dynamically changing the crossover and mutation probabilities to return the evolution to its right track.

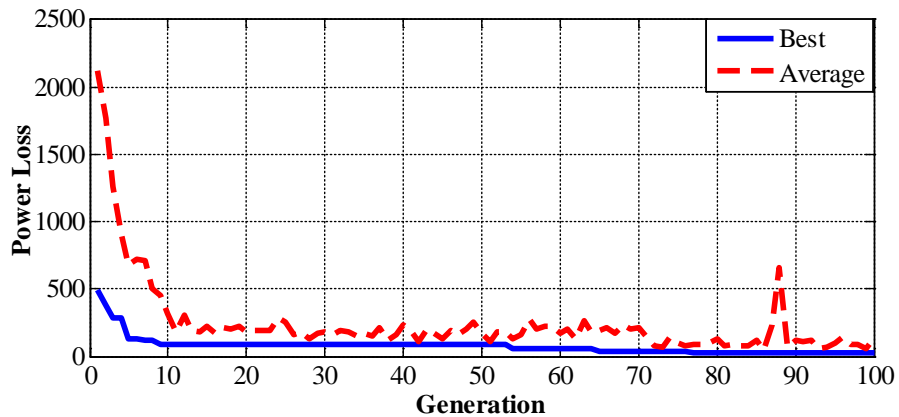


Figure 25: The trend of the average and the best fitness value in each generation

The network configuration of the best found solution, which has the power loss of 28.968 kW, is illustrated in Figure 26 that refers to the chromosome  $Ch1=\{2, 32, 6, 36, 5\}$ . It is notable that the best solution identified in the first generation had the power loss of 492.019 KW that is approximately 17 times higher than the power loss of the best chromosome after 100 generations.

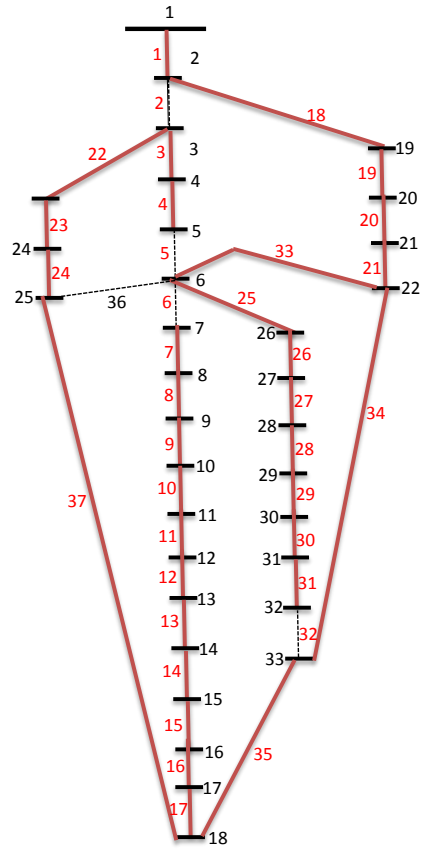


Figure 26: The final solution

A comparison between each branch's power loss of the best identified solution in the first and the final generation is provided in Figure 27. As it can be gathered from the figure, the final solution dramatically wastes less amount of power in all the branches, except Branch #16, compared to the best chromosome identified in the first generation.

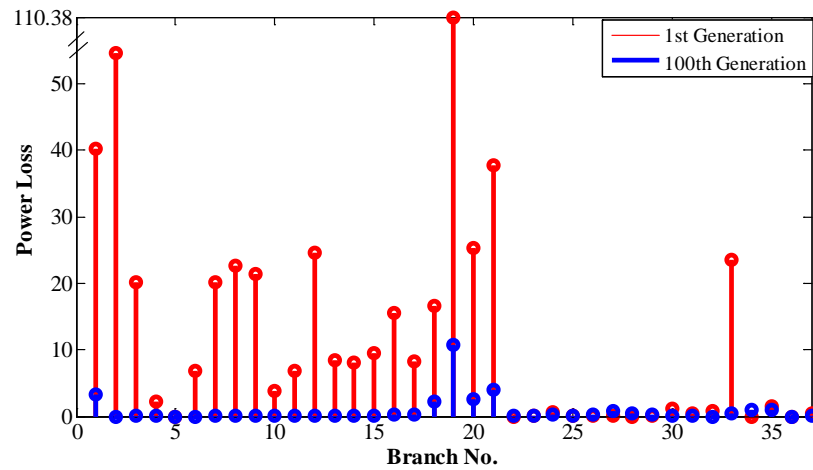


Figure 27: The power loss of each branch

In order to investigate the efficiency of the proposed algorithm in comparison to the that of the classic GA, a trial and error procedure is accomplished to calculate the fixed values of crossover and mutation probability for the classic GA that are  $P_c=0.95$  and  $P_m=0.05$ , respectively. In order to have a fair comparison, the first initial generation of the proposed algorithm which was determined randomly is adopted as the first population of the classic GA. Therefore, it can be claimed that the both algorithms have started their exploitation and exploration from the same start point. After running 100 generations, the best chromosome found by the classic GA is  $Ch2=\{2, 31, 6, 36, 4\}$  that stands for a configuration with the power loss of 52.296 KW. As it can be seen, the identified network by the proposed algorithm wastes 23.328 KW less active power. The trend of average fitness values of the proposed algorithm and that of classic GA is depicted in Figure 28. As it can be observed, not only the average fitness value of the created chromosomes by the proposed algorithm is noticeably less than that of the classic GA, but also the fluctuations of the average fitness values related to the proposed method is



considerably less. It means that the presented dynamic GA with fuzzy crossover and mutation is more robust than the classic GA. Moreover, the chromosomes produced in each generation of the proposed model are more reliable since their power losses are significantly less than that of the configurations identified by the classic GA.

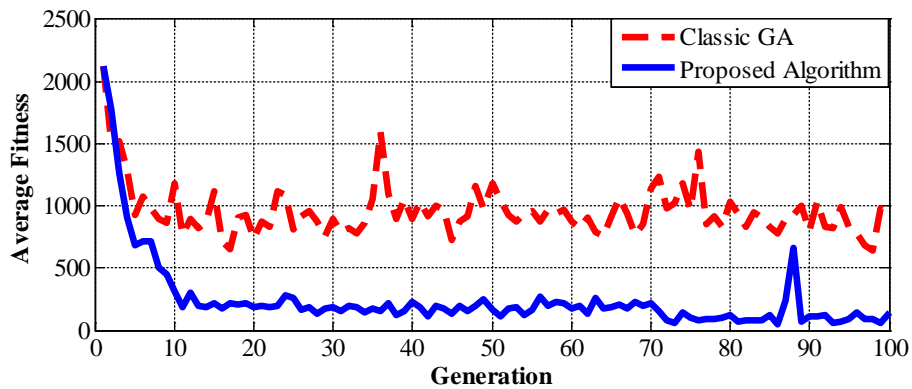


Figure 28: The trend of average fitness values

#### 4.4 Summary

In this chapter, a dynamic fuzzy-based GA is successfully applied to solve the optimization problem of distribution network reconfiguration with the objective function of minimizing total power loss in the system. In order to dynamically tune the probability of crossover and mutation, three fuzzy functions are defined based on the situation of each chromosome, the situation of all the individuals in a population, and finally the age of each chromosome. Simulations of the proposed algorithm are carried on a 33-bus distribution network and the results are compared with the efficiency of the classic GA that utilizes fixed parameters

for the operators of crossover and mutation. The simulation results demonstrate the more robustness and reliability of the proposed algorithm.

# **CHAPTER FIVE: THE IMPACT OF DISTRIBUTED GENERATION INTEGRATION ON OPTIMAL DISTRIBUTION NETWORK RECONFIGURATION**

## **5.1 Methodology**

As it was explained in Chapter 3, Shuffled frog leaping algorithm (SFLA) is a meta-heuristic optimization model that mimics the memetic evolution of a group of frogs looking for the stone containing the maximum food in a swamp. In this chapter the concept of Pareto dominance is considered within the structure of SFLA to develop a multi-objective global optimization model discovering a set of non-dominated solutions located on the optimal Pareto frontier. Figure 29 shows the flowchart of the presented reconfiguration optimization algorithm. More explanations about this flowchart will be provided in the rest of this section.

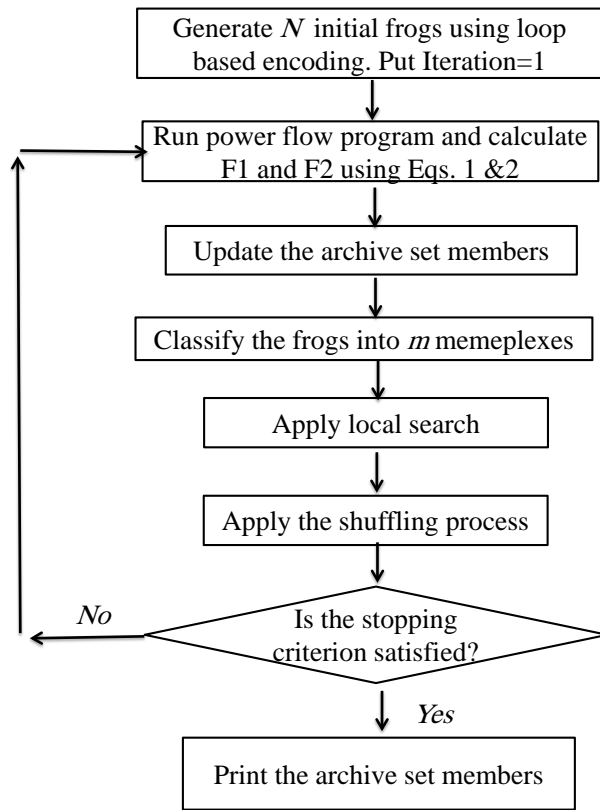


Figure 29: The flowchart of algorithm

The same loop-based encoding technique presented in Chapter 3 is utilized in this chapter as well. In order to implement this encoding strategy, it should be considered that in a radial network the number of closed branches is one unit less than the number of nodes. Also, the number of open branches should be equal to the number of loops in the system. Each encoded network configuration using this technique contains  $P$  bits where  $P$  is the number of loops. Only one open branch should be assigned for each loop. Any loop is not allowed to consist of less than or greater than one open branch. It means each bit of an encoded configuration indicates the branch number of the corresponding loop which is open. For instance, the encoded individual

(i.e. frog) for the network topology shown in Figure 30, which contains 10 nodes, 9 closed branches and 3 loops, is  $F=\{10, 4, 11\}$ .

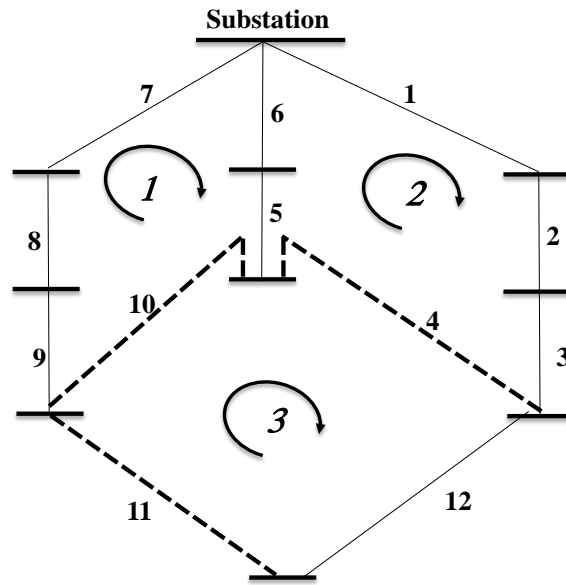


Figure 30: A radial network with three loops

The archive set ( $AS$ ) contains the suboptimal non-dominated solutions during the optimization process. For example, Fig. 31a. shows the  $AS$  members found at iteration  $T$ . As it can be seen, any frog in this set is not able to dominate any other member of  $AS$ . At each iteration  $AS$  members should be updated in two steps: (1) The new generated frogs which are not dominated by the current  $AS$  members should be added to the Pareto frontier. As it can be realized from Figure 31b., the frogs  $z$ ,  $m$  and  $n$  are the new  $AS$  members which are identified at iteration  $T+1$ . (2) The old  $AS$  members which are dominated by the new  $AS$  members should be

removed from the Pareto frontier. As it can be gathered from Figure 31c, the frogs  $x$  and  $y$  which are dominated by the new members  $z$ ,  $m$  and  $n$  are deleted from the archive set.

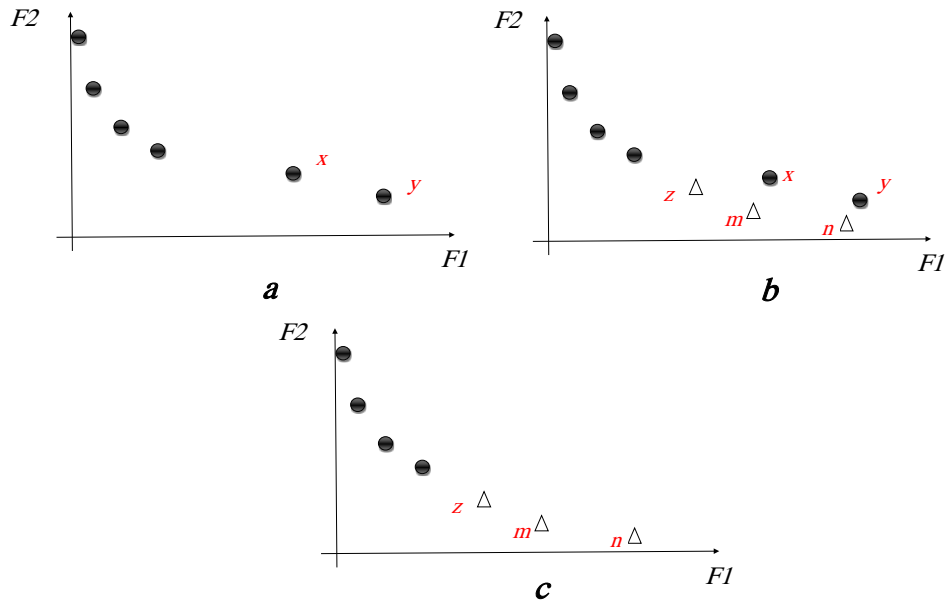


Figure 31: Updating the archive set members

Different methods can be adopted to classify the encoded frogs (i.e. network configurations) into  $m$  memplexes. In this work, a fuzzy based strategy is presented to assign one single fitness value to each frog as a criterion of selection for classifying. The two objective functions defined for the algorithm to be optimized are voltage drop and voltage sag which are formulated in Equations 4 and 15. As it is shown in Figure 32, two fuzzy values are assigned to these objective values using the trapezoidal fuzzy functions. The multiplication of these fuzzy values will yield the fitness value of the corresponding frog. At the next stage, the frogs should

be classified in different memplexes. Roulette wheel method is employed for this purpose. All the memplexes should contain the same number of frogs and they should be prepared fairly consisting of less fertilized and more fertilized frogs. That is why at the beginning step the first member of each memplex should be selected from the roulette wheel so that, most likely, the frogs with higher fitness values will be chosen. When the first members of all the memplexes are selected, this process will be repeated to determine the second members of each memplex, and so on. It should be emphasized that each selected frog should be taken out and it will not be put back in the roulette wheel for further selections.

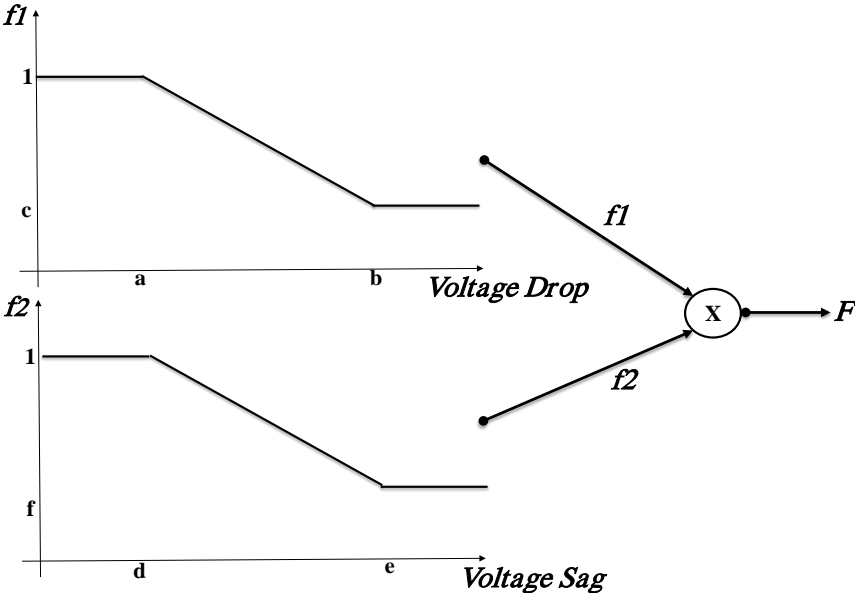


Figure 32: Determining the fitness fuzzy value for classification

Local search is an evolutionary method that is repetitively applied to each memplex to improve the worst frogs of the corresponding memplex. Using Equations 23 and 24, the best and worst frog in the memplex are used to generate a new frog.

If the new frog dominates the worst frog, it will be replaced by  $X_{w,old}$ . Otherwise, this process will be repeated with the difference that instead of Equation 23, Equation 32 will be used in which the best frog among all the memplexes (i.e.  $X_g$ ) will be employed to generate the new frog. If the new developed frog cannot still dominate the older worst frog (i.e.  $X_{w,old}$ ) in the memplex, another frog will be generated randomly to be replaced by the worst frog. It is notable that the worst frog is dominated by the new one when its voltage drop and voltage sag values are higher than that of the new frog. Repeating this evolutionary process for each memplex, the frogs will be improved locally.

$$D = rand().(X_g - X_{w,old}) \quad (32)$$

At the end of each iteration, shuffling process will be applied to make the cultural evolution free from any bias. After improving the worst frogs by Local Search, shuffling processor will combine all the frogs in different memplexes to develop a united population.



## 5.2 Simulation results and discussions

In order to simulate the presented optimization algorithm, MATLAB software is employed on a computer with the processor of Intel(R) Xeon(R) CPU E5-2603 0 @ 1.80 GHz. The reconfiguration model is tested on a 69-bus radial distribution system [63] illustrated in Figure 33 which contains 68 sectionalizing switches and five tie switches. The main transformer is connected to a substation with the nominal power of 100 MVA and the nominal voltage of 12.66 KV. As it is observed from Figure 33, in the initial topology the Branch #69, 70, 71, 72, and 73 are open (i.e.  $F=\{69, 70, 71, 72, 73\}$ ). The stopping criterion of algorithm is to reach iteration #100 while the local search process is repeated 10 times for each memplex in each iteration. Newton-Raphson is utilized as the power flow program. And the points of common coupling (PCC), explained in Chapter 3, for voltage sag calculation are assumed to be Bus #12, 20, 24 and 28.

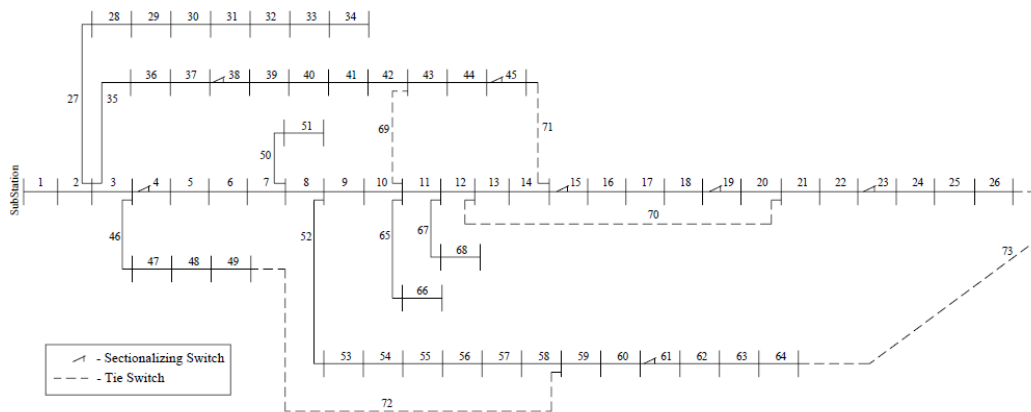


Figure 33: The case study [63]

To study the effect of DG integration, the optimization method is implemented in three different scenarios as is described in Table 6. It is notable that the power factor of all the installed DG units is 0.8 lag.

Table 6: The Description of Different Scenarios

	No. DG units	Location (Bus No.)	Power (KVA)
Scenario #1	0	-	-
Scenario #2	5	11, 21, 50, 55, 61	80, 50, 150, 10, 500
Scenario #3	10	7, 11, 12, 21, 49, 50, 55, 61, 64, 65	15, 80, 80, 50, 150, 150, 10, 500, 100, 30

The number of non-dominated solutions (i.e. the archive set's frogs) increases as the algorithm proceeds since it identifies a higher number of suboptimal configurations located on the Pareto frontier. This growing trend for different scenarios is compared in Figure 34. As it is observed from the figure, approximately, the same number of suboptimal solutions is identified by the algorithm after 100 iterations for the three cases.

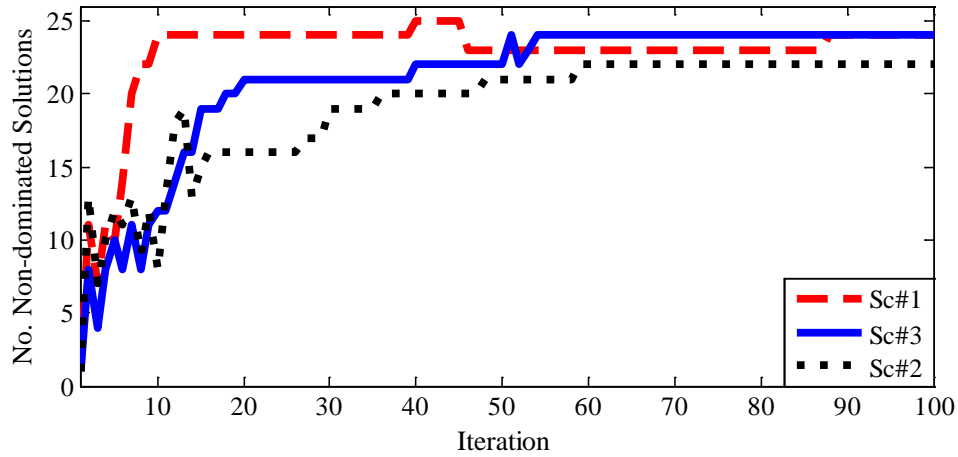


Figure 34: The number of AS members found by the algorithm

The first defined objective function is voltage drop. In order to present the fluctuations of this fitness value during the optimization process, the average voltage drop of all the non-dominated solutions is recorded as the average voltage drop of each iteration. Figure 35 provides a comparison among the declining trends of average voltage drop for three scenarios. This observation verifies that the integration of DG units to the network will improve the performance of optimization algorithm to identify more high-quality suboptimal solutions with less values of voltage drop.

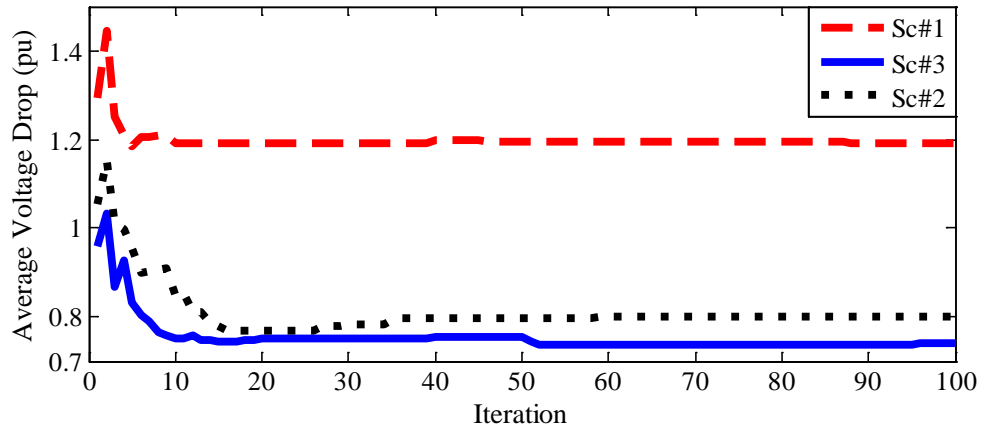


Figure 35: The declining trend of average voltage drop

The second objective function defined for the algorithm is voltage sag. As different non-dominated solutions are found in each iteration, the average voltage sag of suboptimal solutions is recorded to stand for the second fitness value of the relevant iteration. The declining trends of average voltage sag for three scenarios during the optimization process are compared in Figure 36. As it is demonstrated, the presence of DG units in the network will make the optimization algorithm more efficient in finding the topologies with less voltage sag values.

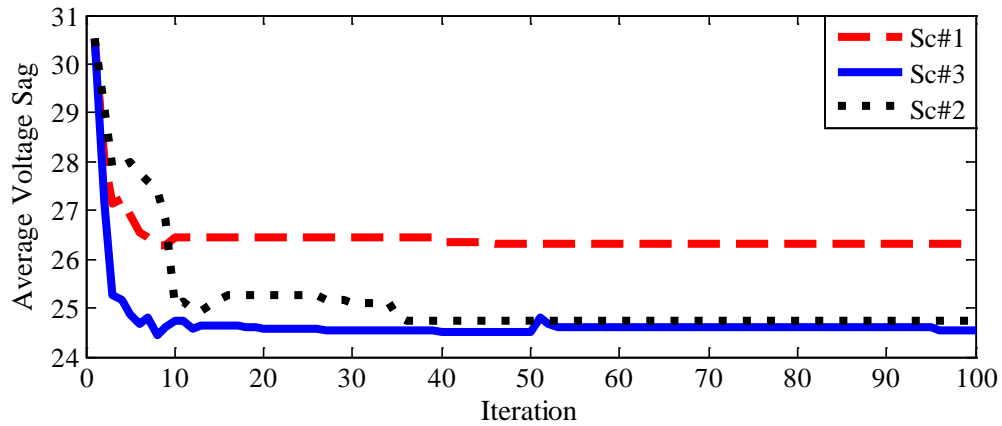


Figure 36: The declining trend of average voltage sag

As it was presented in Figure 34, the algorithm finds approximately the same number of non-dominated solutions after 100 iterations for different scenarios. These suboptimal network configurations are located on Pareto frontiers which are illustrated together in Figure 37. As it was expected, the higher number of DG units in the system will help the reconfiguration model identify more high-quality Pareto frontiers with the lower values of voltage drop and voltage sag.

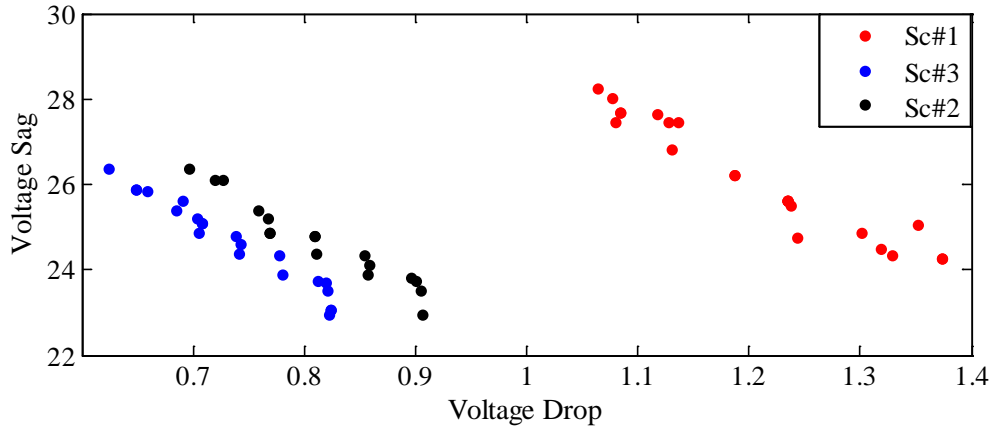


Figure 37: The frontiers identified by the algorithm for three scenarios

Table 7 presents the configurations with the lowest value of voltage drop on the identified frontiers. The second row of this table indicates the open switches of each topology.

Table 7: The Configurations with the Lowest Voltage Drop

	<b>Initial</b>	<b>Scenario #1</b>	<b>Scenario #2</b>	<b>Scenario #3</b>
<i>Configuration</i>	69,70,71,72,73	10, 20, 13, 58, 26	69, 20, 13, 58, 64	69, 19, 13, 58, 64
<i>Voltage Drop</i>	1.8460	1.0637	0.6961	0.6236

The voltage profiles of the network topologies presented in Table 7 are depicted in Figure 38. As it was expected, running the optimization algorithm even in the absence of DG units will lead to a more high-quality suboptimal configuration with an improved voltage profile (refer to the green and red profiles in Figure 38). Also, it is verified that Sc#3 with the highest number of

DG units provides the most desirable voltage profile since the voltage values of different buses are much closer to 1 p.u.

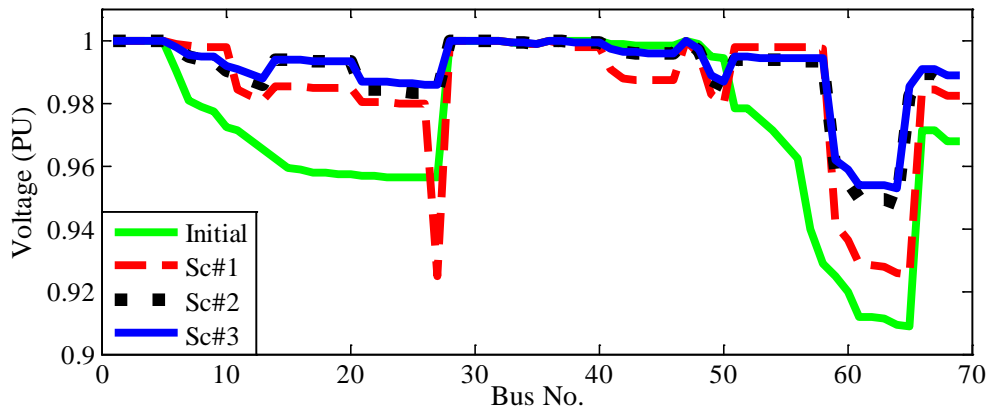


Figure 38: The voltage profile of configurations presented in Table 2

The advantage of employing a Pareto dominance-based optimization algorithm is that the system operator will have the opportunity to pick one of the identified solutions on the Pareto frontier based on the situation of network. If the operator decides to consider an equal importance for voltage drop and voltage sag, the solution located at the center of Pareto frontier will be the best topology for the network. Table 8 shows the configuration and the corresponding fitness values of the solution at the center of Pareto frontiers for three scenarios. As it is demonstrated, the higher number of DG units in the network leads to a higher qualified solution identified by the optimization algorithm.

Table 8: The Configurations Located at the Center of Pareto Frontiers

	<b>Initial</b>	<b>Scenario #1</b>	<b>Scenario #2</b>	<b>Scenario #3</b>
<i>Configuration</i>	69,70,71,72,73	10, 19, 12, 58, 25	69, 19, 12, 58, 26	69, 19, 12, 58, 25
<i>Voltage Drop</i>	1.8460	1.1305	0.7693	0.7406
<i>Voltage Sag</i>	30.9650	26.8401	24.8758	24.3895

As it was gathered from Figure 34, the optimization algorithm identifies 24 non-dominated solutions for Scenario #3, whose fitness values are depicted in Figure 37. Table 9 presents these network topologies. The number in each column indicates the branch number which is open in the corresponding loop.



Table 9: The Suboptimal Configurations Identified for Scenario #3

<i>Solution</i>	<i>Loop#1</i>	<i>Loop#2</i>	<i>Loop#3</i>	<i>Loop#4</i>	<i>Loop#5</i>
<b>1</b>	69	18	12	58	26
<b>2</b>	69	18	12	58	23
<b>3</b>	69	18	12	58	25
<b>4</b>	69	18	12	57	25
<b>5</b>	69	17	12	58	24
<b>6</b>	69	17	12	57	24
<b>7</b>	69	14	12	57	22
<b>8</b>	69	19	13	58	26
<b>9</b>	69	19	12	58	26
<b>10</b>	69	20	13	58	73
<b>11</b>	69	19	12	58	24
<b>12</b>	69	19	12	58	25
<b>13</b>	69	20	14	58	26
<b>14</b>	69	20	13	58	26
<b>15</b>	69	19	12	58	23
<b>16</b>	69	20	12	58	26
<b>17</b>	69	20	12	58	25
<b>18</b>	69	20	12	58	24
<b>19</b>	69	20	13	58	23
<b>20</b>	69	20	12	58	23
<b>21</b>	69	70	12	58	23
<b>22</b>	69	19	13	58	64
<b>23</b>	69	20	13	58	64
<b>24</b>	69	19	12	58	64

### 5.3 Summary

The Pareto-based global optimization algorithm which was proposed in Chapter 3 has been improved in this chapter to solve the multi-objective problem of distribution system reconfiguration with the purpose of optimizing voltage profile and voltage sag. The optimization method utilizes a Pareto dominance technique to recognize non-dominated solutions identified by a shuffled frog leaping algorithm (SFLA) which is adapted in the encoding and partitioning steps. A fuzzy logic is introduced in the partitioning step of SFLA based on the values of voltage drop and voltage sag in order to provide a more accurate criterion for the classification of frogs. The proposed optimization algorithm is implemented in the presence of DGs to step toward the integration of smart grids embedded in the structure of conventional power systems. The simulation results verify that increasing the number and size of added DG units in the network will improve the efficiency of the optimization algorithm to identify higher qualified suboptimal solutions for the system.

## CHAPTER SIX: EXHAUSTIVE SEARCH

Heuristic optimization algorithms do not guarantee to identify the optimal solution. However, they are able to find high-quality suboptimal solutions [64]. As it is discussed in [64], one way to verify the robustness of a heuristic optimization algorithm is to implement it on a smaller case study and compare its performance with the exhaustive search. In this chapter, the efficiency of ASFLA (i.e. adaptive shuffled frog leaping algorithm) is demonstrated by accomplishing the exhaustive search. This algorithm is proposed in Chapter 3 and it has been improved in Chapter 5. In order to implement the exhaustive search, a distribution network with six buses (i.e. nodes) and seven branches is used as the case study which is illustrated in Figure 39. The information of this case study is presented in Tables 10-12.

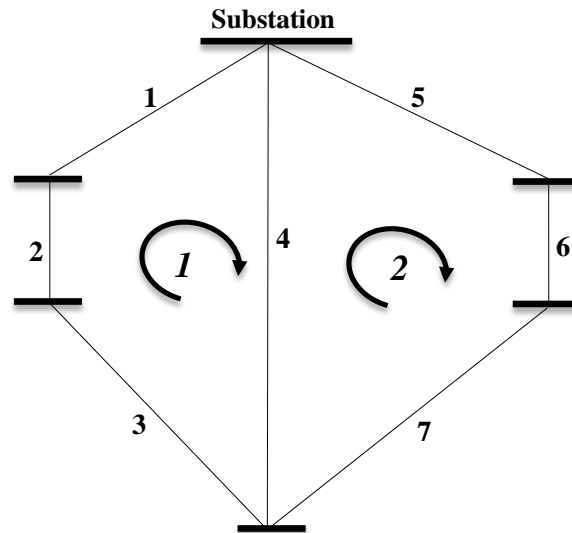


Figure 39: The small case study for exhaustive search

Table 10: Branch Data of the Small Case Study

Branch No.	Bus No. (i)	Bus No. (f)	R (Ohm)	X (Ohm)
1	1	2	0.0005	0.0012
2	2	3	0.5075	0.2885
3	3	4	1.5900	0.5337
4	4	1	0.0251	0.0294
5	5	1	0.0822	0.2011
6	6	5	0.3811	0.1941
7	4	6	0.0044	0.0108

Table 11: Bus Data of the Small Case Study

Bus No.	P (kW)	Q (kVar)
1	0	0
2	1	0.6
3	40.4	30
4	100	72
5	18	13
6	114	81

Table 12: Nonlinear Load Data of the Small Case Study (Percentage of Fundamental Frequency)

Bus No.	Harmonic No.								
	3	5	7	9	11	13	15	17	19
2	0	20	14	0	9	8	0	6	5
4	0	2	1	0	7	6	0	0.3	0.3

It is notable that the exhaustive search evaluates all the possible configurations (i.e.  $2^7=128$ ) and reports the configuration with the best fitness value. And at the next step, the proposed heuristic algorithm (i.e. ASFLA) is simulated to identify the high-quality solutions after 80 iterations. The initial population contains 60 frogs (i.e. 60 initial configurations selected randomly). The number of memplexes is assumed to be three. And for each iteration, the local search step is repeated for 10 times.

As for the first scenario, the exhaustive search is implemented to find the configuration with minimum power loss. The identified configuration is {2,4} where the Branch #2 and Branch #4 are open. After running the proposed ASFLA, it is observed that the same configuration is found after 80 iterations which is depicted in Figure 40.

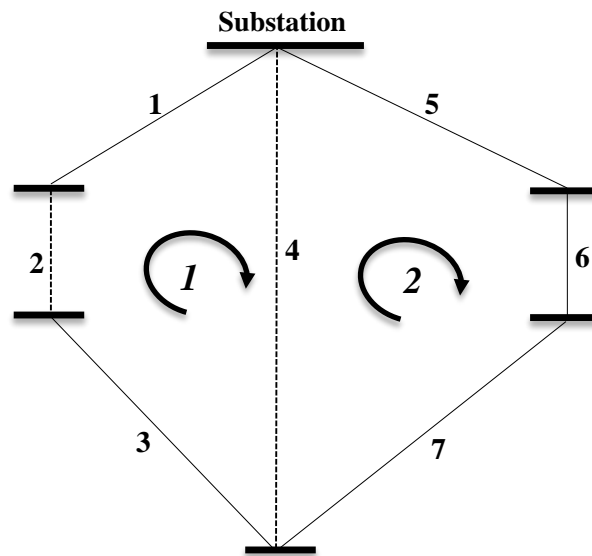


Figure 40: The configuration with minimum power loss

Regarding the second and third scenarios, voltage sag and THD are defined, respectively, as the objective functions. The simulation results verify that the same configurations are identified by exhaustive search and the proposed heuristic algorithm for these scenarios as well. The found solutions for Scenario #1 and Scenario #2 are {1,4} and {2,5}, respectively, which are shown in Figure 41.

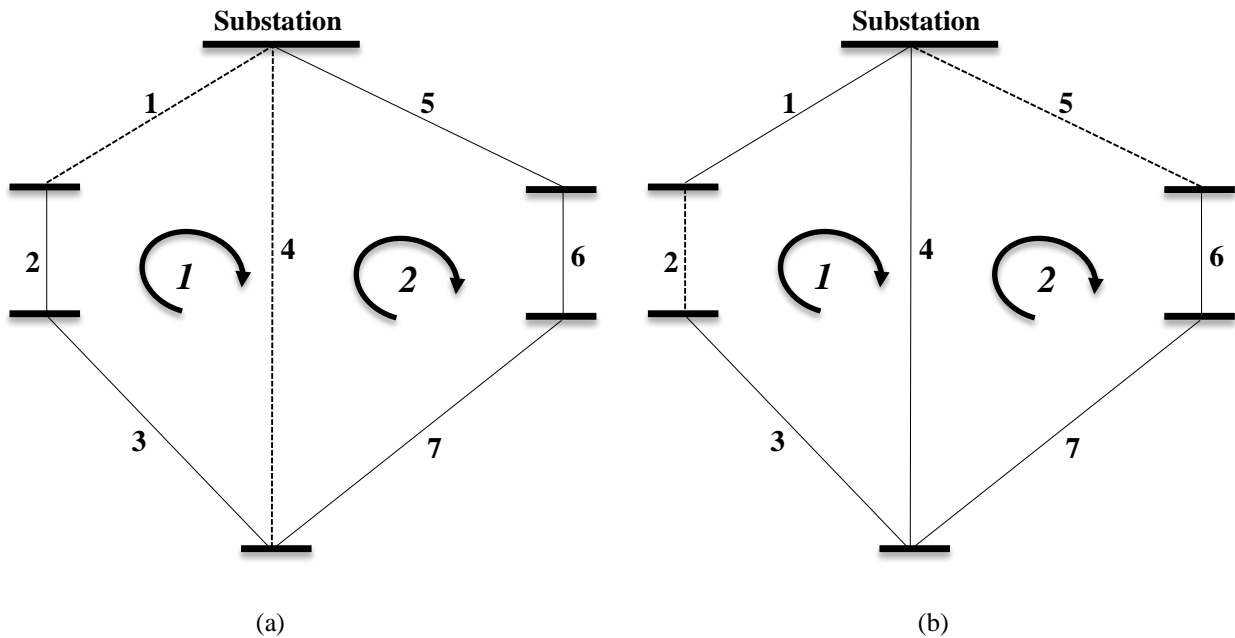


Figure 41: The configurations with (a): minimum voltage sag and (b): minimum THD

It should be emphasized that the presented observation does not guarantee that the proposed heuristic algorithm will have the same efficiency for a distribution system with 3000 branches ( $2^{3000}$  possible configurations). However, it shows that the proposed ASFLA will identify high-quality suboptimal solutions. Once again, it should be mentioned that the declining

trend of the fitness values during the optimization process, which was comprehensively discussed in Chapter 3 and Chapter 5, verifies that the heuristic algorithm is identifying better solutions as the optimization process goes forward.

## CHAPTER SEVEN: CONCLUSION

In the second chapter of this dissertation, a novel optimization power distribution reconfiguration method is proposed that identifies the high-quality suboptimal feasible topologies for large-scale networks with time varying loads. One of the main advantages of the proposed dynamic reconfiguration method is that the optimization process is carried out over a long period of time in contrast to the existing methods that the optimization is re-executed every short period of time.

The proposed method in Chapter 2 is improved in Chapter 4. In the fourth chapter, a dynamic fuzzy-based GA is successfully applied to solve the optimization problem of distribution network reconfiguration with the objective function of minimizing total power loss in the system. In order to dynamically tune the probability of crossover and mutation, three fuzzy functions are defined based on the situation of each chromosome, the situation of all the individuals in a population, and the age of each chromosome.

The problem of multi-objective optimal network reconfiguration which was solved by weighting sum method in Chapter 2, is solved in Chapter 3 by using a Pareto dominance approach to obtain alternative solutions. For the application of multi-objective optimization, this is the main advantage of Pareto dominance techniques over weighted sum method which yields only one solution. Using a Pareto dominance strategy, the operator will have a number of non-dominated solutions bringing about an extra flexibility. Then, based on the condition of the system, the system operator can decide which solution is more appropriate. However, using weighted sum method, the operator needs to rely on the single found solution no matter if it is



suitable for the current situation of the network or not. In the third chapter, a novel hybrid optimization algorithm based on the combination of fuzzy Pareto dominance (FPD) and shuffled frog leaping algorithm (SFLA) is proposed to solve the multi-objective optimization problem of distribution network reconfiguration with the purpose of minimizing power loss, voltage sag and THD.

The Pareto-based global optimization algorithm proposed in Chapter 3 is modified in Chapter 5 to solve the multi-objective problem of distribution system reconfiguration with the purpose of optimizing voltage profile and voltage sag. A fuzzy logic is introduced in the partitioning step of SFLA based on the values of voltage drop and voltage sag in order to provide a more accurate criterion for the classification of frogs. The proposed optimization algorithm is implemented in the presence of DGs to step toward the integration of smart grids embedded in the structure of conventional power systems. The simulation results verify that increasing the number and size of added DG units in the network will improve the efficiency of the optimization algorithm to identify higher qualified suboptimal solutions for the system.

## LIST OF REFERENCES

- [1] A. Merlin and H. Back, "Search for a minimal-loss operating spanning tree configuration in an urban power distribution system," in *Proc. The 5th Power System Computation Conf.*, Cambridge, UK, pp. 1-18, 1975.
- [2] A. A. M. Zin, A. K. Ferdavani, A. B. Khairuddin, and M. M. Naeini, "Reconfiguration of radial electrical distribution network through minimum-current circular-updating-mechanism method," *IEEE Trans. Power Syst.*, vol. 27, no. 2, pp. 968-974, 2012.
- [3] M. R. Farooqi, P. K. Agarwal, and K. R. Niazi, "Multi-objective distribution feeder reconfiguration," *7th WSEAS Int. Conf. Electric Power Systems*, Venice, Italy, pp. 131-138, 2007.
- [4] S. Bahadoorsingh, J. V. Milanovic, Y. Zhang, C. P. Gupta, and J. Dragovic, "Minimization of voltage sag costs by optimal reconfiguration of distribution network using genetic algorithms," *IEEE Trans. Power Delivery*, vol. 22, no. 4, pp. 2271-2278, 2007.
- [5] V. Calderaro, A. Piccolo, and P. Siano, "Maximizing DG penetration in distribution networks by means of GA based reconfiguration," *2005 Int. Conf. Future Power Systems*, Amsterdam, Netherlands, pp. 1-6, 2005.
- [6] A. Coelho, A. B. Rodrigues, and M. G. Da Silva, "Distribution network reconfiguration with reliability constraints," *2004 Int. Conf. Power System Technology (PowerCon 2004)*, Singapore, pp. 1600-1606, 2004.

- [7] A. Mendes, N. Boland, P. Guiney, and C. Riveros, " Switch and tap-changer reconfiguration of distribution networks using evolutionary algorithms," *IEEE Trans. Power Syst.*, vol. 28, no. 1, pp. 85-92, 2013.
- [8] D. Shirmohammadi, "Service restoration in distribution networks via network reconfiguration," *IEEE Trans. Power Delivery*, vol. 7, no. 2, pp. 952-958, 1992.
- [9] H. D. M. Braz and B. A. Souza, "Distribution network reconfiguration using genetic algorithms with sequential encoding: subtractive and additive approaches," *IEEE Trans. Power Syst.*, vol. 26, no. 2, pp. 582-593, 2011.
- [10] B. Enacheanu, B. Raison, R. Caire, O. Devaux, W. Bienia, and N. HadjSaid, "Radial network reconfiguration using genetic algorithm based on the Matroid theory," *IEEE Trans. Power Syst.*, vol. 23, no. 1, pp. 186-195, 2008.
- [11] A. Y. Abdelaziz, S. F. Mekhamer, M. A. L. Badr, F. M. Mohamed, and E. F. El-Saadany, "A modified particle swarm algorithm for distribution systems reconfiguration," *2009 IEEE Power & Energy Society General Meeting (PES)*, Calgary, AB, pp. 1-8, 2009.
- [12] R. S. Rao, S. V. L. Narasimham, M. R. Raju, and A. S. Rao, "Optimal network reconfiguration of large-scale distribution system using harmony search algorithm," *IEEE Trans. Power Syst.*, vol. 26, no. 3, pp. 549-557, 2011.
- [13] J. Olamaei, T. Niknam, and S. B. Arefi, "Distribution feeder reconfiguration for loss minimization based on modified honey bee mating optimization algorithm," *Energy Procedia*, vol. 14, pp. 304-311, 2012.

- [14] A. Y. Abdelaziz, F. M. Mohamed, S. F. Mekhamer, and M. A. L. Badr, "Distribution system reconfiguration using a modified Tabu search algorithm," *Electr. Pow. Syst. Res.*, vol. 80, no. 8, pp. 943-953, Aug. 2010.
- [15] T. Q. D. Khoa and P. T. T. Binh, "A hybrid ant colony search based reconfiguration of distribution network for loss reduction," *2006 IEEE/PES Transmission & Distribution Conf. and Exposition: Latin America*, Caracas, Venezuela, pp. 1-7, 2006.
- [16] Y. J. Jeon, J. C. Kim, J. O. Kim, J. R. Shin, and K. Y. Lee, "An efficient simulated annealing algorithm for network reconfiguration in large-scale distribution systems," *IEEE Trans. Power Delivery*, vol. 17, no. 4, pp. 1070-1078, 2002.
- [17] H. Salazar, R. Gallego, and R. Romero, "Artificial neural networks and clustering techniques applied in the reconfiguration of distribution systems," *IEEE Trans. Power Delivery*, vol. 21, no. 3, pp. 1735-1742, 2006.
- [18] M. A. Kashem, G. B. Jasmon, A. Mohamed, and M. Moghavvemi, "Artificial neural network approach to network reconfiguration for loss minimization in distribution networks," *International Journal of Electrical Power & Energy Systems*, vol. 20, no. 4, pp. 247-258, 1998.
- [19] M. H. Shariatkah and M. R. Haghifam, "Determining of annual distribution feeder configuration using load curves clustering," *16th Conf. Electrical Power Distribution Networks (EPDC)*, Bandar Abbas, Iran, pp. 1-7, 2011.
- [20] C. S. Chen and M. Y. Cho, "Energy loss reduction by critical switches," *IEEE Trans. Power Delivery*, vol. 8, no. 3, pp. 1246-1253, 1993.

- [21] S. A. Yin and C. N. Lu, "Distribution Feeder Scheduling Considering Variable Load Profile and Outage Costs," *IEEE Trans. Power Syst.*, vol. 24, no. 2, pp. 652-660, 2009.
- [22] E. Lopez, H. Opazo, L. Garcia, and P. Bastard, "Online reconfiguration considering variability demand: applications to real networks," *IEEE Trans. Power Syst.*, vol. 19, no. 1, pp. 549-553, 2004.
- [23] T. H. Huynh, "A modified shuffled frog leaping algorithm for optimal tuning of multivariable PID controllers," *2008 IEEE Int. Conf. Industrial Technology (ICIT)*, Chengdu, China, pp. 1-6, 2008.
- [24] M. M. Eusuff, K. Lansey, and F. Pasha, "Shuffled frog-leaping algorithm: a memetic meta-heuristic for discrete optimization," *Engineering Optimization*, vol. 38, no. 2, pp. 129-154, 2006.
- [25] E. Elbeltagi, T. Hegazyb, and D. Grierson, "Comparison among five evolutionary-based optimization algorithms," *Advanced Engineering Informatics*, vol. 19, no. 1, pp. 43-53, 2005.
- [26] E. Alba and B. Dorronsoro, "The exploration/exploitation tradeoff in dynamic cellular genetic algorithms," *IEEE Trans. Evolutionary Computation*, vol. 9, no. 2, pp. 126-142, 2005.
- [27] P. F. le Roux, D. Munda, and Y. Hamam, " Distribution network reconfiguration using genetic algorithm and load flow," *2012 Conference on Power & Energy (IPEC)*, Ho Chi Minh City, Vietnam, vol. 4, pp. 616-620, 2012.

- [28] M. Srinivas and L. M. Patnaik, "Adaptive probabilities of crossover and mutation in genetic algorithms," *IEEE Trans. Systems, Man and Cybernetics*, vol. 24, no. 4, pp. 656-667, 1994.
- [29] J. J. Grefenstette, "Optimization of control parameters for genetic algorithms," *IEEE Trans. Systems, Man and Cybernetics*, vol. 16, no. 1, pp. 122-128, 1986.
- [30] M. Annuziatio and S. Pizzuti, "Adaptive parameterization of evolutionary algorithms driven by reproduction and competition," *2000 European Symp. Intelligent Techniques (ESIT)*, Aachen, Germany, pp. 246-256, 2000.
- [31] M. Last and S. Eyal, "A fuzzy-based lifetime extension of genetic algorithms," *Fuzzy Sets and Systems*, vol. 149, no. 1, pp. 122-128, 2005.
- [32] R. -F. Chang, Y. -C. Chang, and C. -N. Lu, "Feeder reconfiguration for accommodating distributed generations interconnection," *16th Int. Conf. Intelligent System Application to Power Systems (ISAP)*, Hersonissos, Greece, pp. 1-6, 2011.
- [33] R. S. Rao, K. Ravindra, K. Satish, and S. V. L. Narasimham, "Power loss minimization in distribution system using network reconfiguration in the presence of distributed generation," *IEEE Trans. Power Syst.*, vol. 28, no. 1, pp. 317-325, 2012.
- [34] J. -H. Choi, J. -C. Kim, and S. Moon, "Integration operation of dispersed generations to automated distribution networks for network reconfiguration," *IEEE Bologna Power Tech Conf.*, Bologna, Italy, pp. 1-5, 2003.
- [35] H. Nasiraghdama, and S. Jadid,, "Optimal hybrid PV/WT/FC sizing and distribution system reconfiguration using multi-objective artificial bee colony (MOABC) algorithm," *Solar Energy*, vol. 86, no. 10, pp. 3057-3071, 2012.

- [36] Y. Y. Hong, C. Li, and S. Y. Ho, "Determination of network configuration considering multiobjective in distribution systems using genetic algorithms," *IEEE Trans. Power Syst.*, vol. 20, no. 2, pp. 1062-1069, 2005.
- [37] F. R. Dávalos and M. R. Irving, "The edge-set encoding in evolutionary algorithms for network reconfiguration problems in power distribution systems," *16th Power Systems Computation conf. (PSCC)*, Glasgow, Scotland, pp. 1-7, 2008.
- [38] E. G. Carrano, C. M. Fonseca, R. H. C. Takahashi, L. C. A. Pimenta, and O. M. Neto, "A preliminary comparison of tree encoding schemes for evolutionary algorithms," *2007 IEEE Int. Conf. Systems, Man and Cybernetics (ISIC)*, Montreal, Que, pp. 1969-1974, 2007.
- [39] J. R. Kim, K. H. Do, and W. Y. Chung, "A new encoding method-based genetic algorithm for solving OCST problems," in *Proc. 8th Int. Symposium on Advanced Intelligent Systems (ISIS)*, Sokcho-City, Korea, pp. 630-635, 2007.
- [40] Y. Y. Hong, C. Li, and S. Y. Ho, "The Dandelion code: a new coding of spanning trees for genetic algorithms," *IEEE Trans. Evolutionary Computation*, vol. 11, no. 1, pp. 91-100, 2007.
- [41] E. Alba and J. M. Troya, "A survey of parallel distributed genetic algorithms," *Complexity*, vol. 4, no. 4, pp. 31-52, 1999.
- [42] V. S. Gordon and D. Whitley, "Serial and parallel genetic algorithms as function optimizers," in *Proc. 5th Int. Conf. Genetic Algorithms (ICGA)*, Urbana-Champaign, IL, pp. 177-183, 1993.

- [43] S. C. Lin, W. F. Punch, and E. D. Goodman, "Coarse-grain parallel genetic algorithms: categorization and new approach," in *Proc. 6th IEEE Symposium on Parallel and Distributed Processing*, Dallas, TX, pp. 28-37, 1994.
- [44] T. C. Belding, "The distributed genetic algorithm revisited," in *Proc. 6th Int. Conf. Genetic Algorithms*, San Francisco, CA, pp. 122-129, 1995.
- [45] D. Lim, Y. S. Ong, Y. Jin, B. Sendhoff, and B. S. Lee, "Efficient hierarchical parallel genetic algorithms using grid computing," *Future Generation Computer Systems*, vol. 23, no. 4, pp. 658-670, 2007.
- [46] R. S. Rao, K. Ravindra, K. Satish, and S. V. L. Narasimham, "Adaptive probabilities of crossover and mutation in genetic algorithms," *IEEE Trans. Systems, Man and Cybernetics*, vol. 24, no. 4, pp. 656-667, 1994.
- [47] V. Delpoit and D. Liesch, "Fuzzy-c-mean algorithm for codebook design in vector quantisation," *Electronics Letters*, vol. 30, no. 13, pp. 1025-1026, 1994.
- [48] W. Cai, S. Chen, and D. Zhang, "Fast and robust fuzzy c-means clustering algorithms incorporating local information for image segmentation," *Pattern Recognition*, vol. 40, no. 3, pp. 825-838, 2007.
- [49] D. Zhang, Z. Fu, and L. Zhang, "An improved TS algorithm for loss-minimum reconfiguration in large-scale distribution systems," *Electr. Pow. Syst. Res.*, vol. 77, no. 5-6, pp. 685-694, 2007.
- [50] P. Heine and M. Lehtonen, "Voltage sag distributions caused by power system faults," *IEEE Trans. Power Syst.*, vol. 18, no. 4, pp. 1367-1373, 2003.



- [51] N. Farokhnia, H. Vadizadeh, S. H. Fathi, and F. Anvariasl, "Calculating the formula of line-voltage THD in multilevel inverter with unequal dc sources," *IEEE Trans. Industrial Electronics*, vol. 58, no. 8, pp. 3359-3372, 2011.
- [52] A. Vescan, "Pareto Dominance-based approach for the component selection problem," *2nd UKSIM European Symposium on Computer Modeling and Simulation*, Liverpool, UK, pp. 58-63, 2008.
- [53] S. Benedict and V. Vasudevan, "Fuzzy-Pareto-Dominance and its application in evolutionary multi-objective optimization," *EMO'05 Proc. 3rd int. conf. Evolutionary Multi-Criterion Optimization*, Berlin, Germany, pp. 399-412, 2005.
- [54] F. R. Davalos and M. R. Irving, "The edge-set encoding in evolutionary algorithms for network reconfiguration problems in power distribution systems," *16th Power Systems Computation conf. (PSCC)*, Glasgow, Scotland, pp. 1-7, 2008.
- [55] W. M. Lin and M. T. Tsay, " Distribution feeder reconfiguration with refined genetic algorithm," *IEE Proc. Gen. Trans. Distr*, vol. 147, no. 6, pp. 349-354, 2000.
- [56] M. M. Eusuff and K. E. Lansey, "Optimization of water distribution network design using the shuffled frog leaping algorithm," *Water Resour. Plan Manage*, vol. 129, no. 3, pp. 210-225, 2003.
- [57] J. R. S. Mantovani, F. Casari and R. A. Romero, "Reconfiguration of Radial Distribution Systems Using the Voltage Drop Criteria," *Control and Automation Magazine, Creative Commons License, SBA*, vol. 11, no. 3, pp. 150-159, 2000.
- [58] M. Melanie, "An introduction to genetic algorithms," Fifth edition, 1999.

- [59] M. Last and S. Eyal, "A fuzzy-based lifetime extension of genetic algorithms," *Fuzzy Sets and Systems*, vol. 149, no. 1, pp. 122-128, 2005.
- [60] S. H. Ling, F. H. F. Leung, H. K. Lam, Y. -S. Lee, and P. K. S. Tam, "A novel genetic-algorithm-based neural network for short-term load forecasting," *IEEE Trans. Industrial Electronics*, vol. 50, no. 4, pp. 793-799, 2003.
- [61] W. -Y. Lin, W. -Y. Lee, and T. -P. Hong, "Adapting crossover and mutation rates in genetic algorithms," *Journal of information science and engineering*, vol. 19, pp. 889-903, 2003.
- [62] M. E. Baran and F. F. Wu, "Network reconfiguration in distribution systems for loss reduction and load balancing," *IEEE Trans. Power Delivery*, vol. 4, no. 2, pp. 1401-1407, 1989.
- [63] N. C. Sahooa and K. Prasad, "A fuzzy genetic approach for network reconfiguration to enhance voltage stability in radial distribution systems," *IEEE Energy Conversion and Management*, vol. 47, pp. 3288-3306, Nov. 2006.
- [64] H. P. Schmidt, N. Ida, N. Kagan, and J. C. Guaraldo, "Fast reconfiguration of distribution systems considering loss minimization," *IEEE Trans. Power Syst.*, vol. 20, no. 3, pp. 1311-1319, 2005.